# Highlights

- 1. Conifers add leaf wax *n*-alkanes to sediments when they dominate the landscape
- 2. Some conifer taxa provide subtly different *n*-alkane chain length patterns
- 3. Relative abundance of *n*-alkanes/terpenoids qualitatively relate to paleovegetation
- 4. Plant terpenoid  $\delta^{13}$ C values can be used to detect the source of *n*-alkanes
- 5. n-Alkanes from conifers can be 2–6‰  $^{13}$ C-enriched than those from angiosperms

Conifers are a major source of sedimentary leaf wax *n*-alkanes when dominant in the landscape: Case studies from the Paleogene Kristen M. Schlanser<sup>a,\*</sup>, Aaron F. Diefendorf<sup>a</sup>, Christopher K. West<sup>b</sup>, David R. Greenwood<sup>c</sup>, James F. Basinger<sup>b</sup>, Herbert W. Meyer<sup>d</sup>, Alexander J. Lowe<sup>e</sup>, Hans H. Naake<sup>a</sup> <sup>a</sup>Department of Geology, University of Cincinnati, Cincinnati, OH 45221, USA <sup>b</sup>Department of Geological Sciences, University of Saskatchewan, 114 Science Place, Saskatoon, SK, S7N 5E2, Canada <sup>c</sup>Department of Biology, Brandon University, 270 18<sup>th</sup> Street, Brandon, MB, R7A 6A9, Canada <sup>d</sup>National Park Service, Florissant Fossil Beds National Monument, Florissant, P.O. Box 185, CO 80816, USA <sup>e</sup>Department of Biology, University of Washington, 24 Kincaid Hall, Seattle, WA 98195 USA \*Corresponding author (K.M. Schlanser): kschlans@gmail.com 

# **ABSTRACT**

24

25

26

27

28

29

30

31

32

33

34

35

36

37

38

39

40

41

42

43

44

45

Plant wax *n*-alkanes are valuable paleoclimate proxies because their carbon ( $\delta^{13}$ C) and hydrogen  $(\delta^2 H)$  isotopes track biological and environmental processes. Angiosperms produce higher concentrations of *n*-alkanes than conifers, with some exceptions. Vegetation source is significant because in similar climates, both taxa produce *n*-alkanes with unique  $\delta^{13}$ C and  $\delta^{2}$ H values due to different physiological strategies. To test whether conifers contribute significantly to sediment nalkanes and result in distinctive isotopic signatures, we collected sediment samples from a suite of Paleogene paleobotanical sites in North America with high and low conifer abundances. To disentangle the source of sediment n-alkanes, we measured the  $\delta^{13}$ C values of nonsteroidal triterpenoids (angiosperm biomarkers) and tricyclic diterpenoids (conifer biomarkers) to determine angiosperm and conifer end member  $\delta^{13}$ C values. We then compared these end member values to *n*-alkane  $\delta^{13}$ C values for each site to estimate their major taxon sources. At sites dominated by conifer macrofossils,  $\delta^{13}$ C values of *n*-alkanes indicate a conifer source. At mixed conifer and angiosperm sites, conifer contributions increased with increasing *n*-alkane chain length. At sites where conifers were not as abundant as angiosperms, the  $\delta^{13}$ C values of nalkanes indicate a predominant angiosperm source with some sites showing a conifer contribution to n-C<sub>33</sub> and n-C<sub>35</sub> alkanes. This suggests that conifers in the Paleogene contributed to longer chain n-alkanes (n- $C_{33}$  and n- $C_{35}$ ) even when not the dominant taxa, but this likely differs for other geographic locations and taxa. This new approach allows unique floral information to be extracted when chain length is carefully considered in the absence of other paleobotanical data and necessitates having some paleovegetation constraints when interpreting carbon and hydrogen isotopes of plant wax-derived *n*-alkanes.

46

- 47 Keywords: plant biomarkers; terpenoids; organic geochemistry; North America; Arctic;
- 48 Florissant; paleobotany; Paleogene; fossil leaves; carbon isotopes

49

50

51

52

53

54

55

56

57

58

59

60

61

62

63

64

65

66

67

68

69

### 1. Introduction

Long chain *n*-alkanes ( $\geq C_{25}$ ) are acyclic, saturated hydrocarbons produced by plants and are a major constituent of cuticular leaf waxes. The carbon ( $\delta^{13}$ C) and hydrogen ( $\delta^{2}$ H) isotopic compositions of leaf wax *n*-alkanes are sensitive to biological and environmental processes, making them useful plant biomarkers when preserved as molecular fossils in the geologic record (Meyers, 1997; Sauer et al., 2001; Castañeda and Schouten, 2011; Diefendorf and Freimuth, 2017). The  $\delta^{13}$ C values of leaf wax *n*-alkanes have been used to infer fluctuations in the carbon cycle (Smith et al., 2007; Tipple et al., 2011), as paleovegetation indicators (Magill et al., 2013; Garcin et al., 2014), and in other paleoclimate applications (Reichgelt et al., 2016; Bush et al., 2017). Likewise,  $\delta^2$ H values have been applied to reconstruct paleohydrology and track changes in aridity (Pagani et al., 2006; Polissar and Freeman, 2010; Sachse et al., 2012; Baczynski et al., 2017) and to infer paleoaltimetry (Polissar et al., 2009; Hren et al., 2010; Feakins et al., 2018). Despite the widespread use of sediment leaf wax *n*-alkanes in the geologic community, the vegetation source of these plant biomarkers in sediments is often unresolved because both conifers and angiosperms produce *n*-alkanes (Otto et al., 2005; Schouten et al., 2007; Smith et al., 2007). Modern studies show that conifers common to North America over the past 66 million years have produced significantly less (up to 200×) *n*-alkanes than woody angiosperm species (Diefendorf et al., 2011; Bush and McInerney, 2013). However, there are nuances between the different chain lengths and taxa. Pinaceae produce only minor amounts of *n*-alkanes (Diefendorf et al., 2015b) whereas some Cupressaceae (the cypress family), such as Cupressoideae and

Callitroideae, and some Taxodioideae, can produce significant amounts of *n*-alkanes, especially C<sub>33</sub> and C<sub>35</sub> chain lengths (Diefendorf et al., 2015b). Other conifer groups such as Podocarpaceae and Araucariaceae produce large amounts of *n*-C<sub>29</sub> and *n*-C<sub>31</sub> alkanes, but are uncommon or absent in North America in the last 66 Ma. Many landscapes in North America today are dominated by conifers of Pinaceae and/or Cupressaceae, including boreal forests (taigas), the coastal forests of the Pacific Northwest, and the coastal swamps of southeastern North America, and their distributions have waxed and waned in the past (Leslie et al., 2012; Lane, 2017; Lane et al., 2018). If conifers are abundant on the landscape, it may be problematic to assume *n*-alkanes are ubiquitously angiosperm-derived in modern or geologic sediments.

Otto et al. (2005) analyzed plant biomarkers from angiosperm and conifer fossil leaves preserved in the Miocene Clarkia Formation, Idaho, USA and reported that angiosperm leaves contained higher abundances of *n*-alkanes than the conifer fossil leaves. In another study from several Paleocene and Eocene fossil leaf sites in the Bighorn Basin, Wyoming the ratios of diterpenoids (conifer biomarkers) to *n*-alkanes were similar to the ratio of conifers to angiosperms documented by the macrofossils, providing evidence that sediment *n*-alkanes at these sites were also largely derived from angiosperms (Diefendorf et al., 2014). However, these studies represent sites with abundant angiosperms. In the Paleogene of North America, the preservation of conifer-dominated environments is less common, but one notable example is the High Arctic during the late Paleocene and early Eocene. Here, low-lying areas were frequently dominated by deciduous conifer swamp forests of *Metasequoia* and *Glyptostrobus*, as evidenced by an abundance of macrofossil and pollen data (Greenwood and Basinger, 1994; McIver and Basinger, 1999; Harrington et al., 2012; West et al. 2019). These sites are especially important as climate analogs for future warming (Burke et al., 2018). Other sites include the early Eocene

Okanagan Highlands, British Columbia, Canada (i.e., Falkland and Driftwood Canyon) with abundant deciduous and evergreen Cupressaceae and Pinaceae conifers (Greenwood et al., 2005, 2016; Smith et al., 2012; Eberle et al., 2014), and the Oligocene Creede, Colorado that captures a high-elevation evergreen conifer-dominated environment of *Juniperus* and Pinaceae (Wolfe and Schorn, 1990). When conifers make up substantial components of the landscape, this raises questions about how this affects the source of leaf wax n-alkanes in the preserved sediments; and if conifers are contributing significantly to leaf wax n-alkanes, then how are the  $\delta^{13}$ C and  $\delta^{2}$ H values affected?

93

94

95

96

97

98

99

100

101

102

103

104

105

106

107

108

109

110

111

112

113

114

115

While both angiosperms and conifers produce *n*-alkanes, these two plant groups have different  $\delta^{13}$ C and  $\delta^{2}$ H distributions, even in similar environments (Diefendorf et al., 2010; 2011). Conifers generally tend to have higher  $\delta^{13}$ C values than angiosperms due to differences in physiology and water use efficiency strategies (Brooks et al., 1997; Pedentchouk et al., 2008; Leonardi et al., 2012). The ability to investigate the paleovegetation source of *n*-alkanes is currently lacking. One consequence of this has led to different interpretations for the magnitude of the carbon isotope excursion (CIE) during the Paleocene-Eocene Thermal Maximum (PETM), an abrupt warming event (Pagani et al., 2006; Schouten et al., 2007). In the Arctic, Pagani et al. (2006) recorded a CIE of 4.5% from *n*-alkanes assumed to be derived entirely from angiosperms. From the same Arctic marine core, Schouten et al. (2007) showed that the CIE varied from 3‰ in diterpenoids, derived from conifers, to 6‰ in triterpenoids (angiosperm biomarkers) and thus argues that the *n*-alkanes are actually recording a mixed vegetation signal. In the Bighorn Basin, Wyoming, Smith et al. (2007) documented a 4.6% CIE from *n*-alkanes, also best interpreted as angiosperm-derived. Nevertheless, Diefendorf et al. (2011) estimated that the CIE could be as high as 5.6% in the Bighorn Basin if *n*-alkanes were derived from a mixed

source of angiosperms and conifers. This underscores why it can be necessary to constrain vegetation when interpreting carbon and hydrogen isotopes in paleo applications. We are currently lacking a method that can identify the vegetation source of *n*-alkanes in the geologic record, especially in the absence of fossil data.

Here we investigate a possible strategy to infer the major taxon sources of sediment nalkanes using paleobotanical sites in North America from the Paleogene that capture a range of forest types, with high, mixed, and low conifer abundance. First, we examine organic proxies that have been commonly used in geologic studies as paleoenvironmental and paleovegetation to identify possible correlations between sites with high and low conifer abundances. Then we compare the relative abundances and  $\delta^{13}$ C values of *n*-alkanes to conifer- and angiospermderived terpenoids. Tricyclic diterpenoids are produced almost exclusively by gymnosperms. Nonsteroidal pentacyclic triterpenoids and their degradation products (e.g., des-A compounds) are diagnostic of angiosperms (Stout, 1992; Killops et al., 1995; Otto et al., 1997; Diefendorf et al., 2019). We utilize the  $\delta^{13}$ C values preserved in terpenoids as vegetation end members, as these values are sensitive to vegetation source (Diefendorf et al., 2012) and are not significantly altered by post-depositional processes (Freeman and Pancost, 2013; Diefendorf et al., 2015a). By using the  $\delta^{13}$ C values of terpenoids as conifer and angiosperm end member values, we provide a framework for considering the source of *n*-alkanes from other sites and times dominated by conifers, a division of gymnosperms. We propose that the *n*-alkanes can be derived from conifers when abundant on the landscape, and that longer chain homologues (C<sub>33</sub>, C<sub>35</sub>) can be coniferspecific biomarkers even in locations where the macro- or microfossil floras are not dominated by conifers.

116

117

118

119

120

121

122

123

124

125

126

127

128

129

130

131

132

133

134

135

136

137

#### 2. Methods

139

140

141

142

143

144

145

146

147

148

149

150

151

152

153

154

155

156

157

158

159

160

161

2.1. Sites and paleobotanical information

Sediment samples were collected from Paleogene fossil leaf sites across North America previously characterized by paleobotanical studies to encompass fossil localities with both high and low conifer relative abundances as compared to angiosperms in terms of preserved biomass (Fig. 1; Table 1). Localities with a high abundance of conifers include sites spanning the late Paleocene to early and middle Eocene of Ellesmere and Axel Heiberg islands in the Canadian Arctic, early Eocene Driftwood Canyon in British Columbia, Canada, and the Oligocene Creede Formation in Colorado, USA. Localities with lower abundances of conifers relative to angiosperms include Paleocene and Eocene Bighorn Basin sites in Wyoming, USA and late Eocene Florissant Fossil Beds National Monument, Colorado, USA. We measured the abundances and  $\delta^{13}$ C values of *n*-alkanes and terpenoids from all locations except for the Bighorn Basin. For Bighorn Basin sites, terpenoid and *n*-alkane abundances were reported in Diefendorf et al. (2014) and their respective  $\delta^{13}$ C data were presented by Diefendorf et al. (2015a). On Ellesmere Island, samples were collected from outcrops of the upper Paleocene and lower Eocene Margaret and Mount Moore formations, including Hot Weather Creek, Fosheim Anticline, Stenkul Fiord, Split Lake, Lake Hazen, Mosquito Creek, Strathcona Fiord, and Boulder Hills. On Axel Heiberg Island, samples were collected from outcrops of the middle Eocene Buchanan Lake Formation from sites at the Fossil Forest of the Geodetic Hills. During the late Paleocene and through the middle Eocene, the Arctic was temperate with mean annual temperatures (MAT) ranging from 7.6 °C to 12.9 °C, with mild winters, high mean annual precipitation (MAP) between 1310 and 1800 mm/year, and relatively high humidity

across the various paleobotanical sites (Eberle et al., 2010; Greenwood et al., 2010; Eberle and Greenwood, 2012; West et al., 2015; 2020). The landscape was a mosaic of floodplains, swamps, and upland environments (McIver and Basinger, 1999; Eberle and Greenwood, 2012). Samples were collected from floodplain depositional environments with the exception of one sample from Stenkul Fiord which was collected from a coal swamp. Floodplains are represented by fossiliferous mudstones and siltstones. Deciduous conifers dominated the wetter sites, while mixed deciduous conifer and angiosperm flora inhabited the floodplains characterized by siltstones. Macrofossil and pollen data from the Paleocene and early Eocene indicate deciduous conifers such as *Metasequoia* and *Glyptostrobus* (Cupressaceae) were abundant while evergreen conifers were relatively rare (McIver and Basinger, 1999). Some of the more common angiosperms during this time include Ushia, Trochodendroides, Ulmus, Archeampelos, Aesculus, Corylites, Intratriporopollenites, Ailanthipites fluens, Aesculiidites sp., Mediocolpopollis sp., and Diervilla, but species and abundances vary by site (Harrington et al., 2012; West et al., 2019). During the middle Eocene, the paleofloras became more diverse and evergreen conifers increased in diversity and abundance. Swamps and wetlands were still dominated by Metasequoia and Glyptostrobus, but other locally abundant conifers were Larix, Pseudolarix, Picea, Tsuga, Chameacyparis, Taiwania, and Pinus (Greenwood and Basinger, 1994; McIver and Basinger, 1999; Eberle and Greenwood, 2012). Commonly preserved angiosperms from these middle Eocene sites include Alnus, Betula, Magnolia, Platanus, Quercus, Trochodendroides, and Juglandaceae (McIver and Basinger, 1999; Eberle and Greenwood, 2012; Harrington et al., 2012). Samples collected at the Driftwood Canyon Provincial Park in British Columbia come

from an unnamed formation in the lower Eocene Ootsa Lake Group. The outcrop consists

162

163

164

165

166

167

168

169

170

171

172

173

174

175

176

177

178

179

180

181

182

183

184

principally of finely bedded lacustrine shales to silty sandstones, with minor coals and interbedded volcanic ashes, and represent a rarely preserved upland environment (Greenwood et al., 2016). Sediments were deposited during the Early Eocene Climatic Optimum when the region was experiencing a period of active volcanism (MacIntyre et al., 2001). MAT is estimated to be ~10–15 °C with minimal, if any, freezing during colder months and MAP of ~1160 mm/yr (Greenwood et al., 2005). Macroflora and palynology indicate this location was a mixed coniferbroadleaf forest. Pollen data show Abies and Pseudolarix (Pinaceae) as the dominant conifers at this site (Moss et al., 2005). However, macrofossils present a much greater diversity of conifers, with Metaseguoia, Seguoia, Chamaecyparis, and Thuja common, and with lesser amounts of Abies, Larix, Picea, Pinus, Pseudolarix, and rare instances of the non-conifer gymnosperm Ginkgo (Greenwood et al., 2005). The most common broadleaf deciduous angiosperms include Alnus, Betula, Sassafrass, Ulmus, and Fagaceae as indicated by pollen and leaf fossils (Moss et al., 2005; Greenwood et al., 2016). Conifer and angiosperm compositions are highly variable within individual beds. These short-term fluctuations in relative abundances are attributed to successional processes in response to nearby volcanic eruptions and fires, and to local physical and hydrological changes as the regional landscape evolved.

185

186

187

188

189

190

191

192

193

194

195

196

197

198

199

200

201

202

203

204

205

206

207

Samples collected from outcrops of the upper Oligocene Creede Formation represent < 1 Myr of lacustrine sedimentary deposition within a moat lake that had formed inside a collapsed caldera with a resurgent dome. The lake was cold, permanently stratified, and likely had bicarbonate-rich water (Larsen and Crossey, 1996). This locality had a cool, montane climate. Various paleobotanical methods used as paleoclimate proxies have estimated MAT ranging from 0 °C to 9 °C (Wolfe and Schorn, 1989; Leopold and Zaborac-Reed, 2014; 2019) and MAP from 437 to 635 mm/yr (Wolfe and Schorn, 1989; Barton, 2010). Precipitation was likely seasonal,

with dry summers and wet winters. The macroflora resembles a mixed coniferous community ranging from closed forests to woodlands to chaparral environments (Wolfe and Schorn, 1989). 

Juniperus (Cupressaceae) makes up roughly half of the conifer remains at Creede. Other conifer taxa include Abies, Picea, and Pinus (Pinaceae). Among the angiosperms, which are comparatively uncommon at Creede, the most abundant is the shrub Cercocarpus (mountain mahogany) of the Rosaceae (Wolfe and Schorn, 1989). Other angiosperm families represented at Creede include Berberidaceae, Salicaceae, Philadelphaceae, Grossulariaceae, Fabaceae, and Bignoniaceae.

In the Bighorn Basin, samples were collected from carbonaceous beds of the Paleocene and lower Eocene Fort Union and Willwood formations and represent floodplain depositional environments. Paleocene sites include Grimy Gulch, Belt Ash, Cf-1, Honeycombs, and Latest Paleocene site and Eocene sites include WCS7, Dorsey Creek Fence, and Fifteenmile Creek. The climate was warm during the Paleocene and Eocene, with MAT ranging from 10.5 to 22 °C and MAP from 1090 mm/yr to 1730 mm/yr at the various sites (Diefendorf et al., 2015a). Fossil flora collected from these beds represent mixed broadleaf and conifer forests dominated by angiosperms. *Metasequoia* and *Glyptostrobus* were the most common conifers at these sites, when present, with minor amounts of other Cupressaceae (Diefendorf et al., 2015a).

Angiosperms at these sites were diverse and represent such groups as Betulaceae, Cercidiphyllaceae, Cornaceae, Fagaceae, Juglandaceae, Lauraceae, Magnoliaceae, Malvaceae, Platanaceae, Salicaceae, and Zingiberaceae (Hickey, 1980; Wing, 1980, 1984; Wing et al., 1995; Davies-Vollum and Wing, 1998; Currano et al., 2008; Currano, 2009; Diefendorf et al., 2014).

Formation at Florissant Fossil Beds National Monument represent sediments from a lacustrine

Samples collected from outcrops of the middle shale unit of the upper Eocene Florissant

environment. The samples consist of mudstones and finely laminated shales and tuffaceous beds. At times during the deposition, the lake was a closed system along an elongated paleo-valley dammed by volcanic sediments (Buskirk et al., 2016). Well-preserved laminations indicate the lake was permanently stratified (McLeroy and Anderson, 1966). Macrofossil and pollen data suggest this area had seasonal rainfall, mild winters, and a warm temperate climate (Leopold and Clay-Poole, 2001; Allen et al., 2020). MAT and MAP are estimated using various paleobotanical methods as paleoclimate proxies and range from 11 °C to 18 °C and MAP about 700 mm/year (Gregory, 1994; Leopold and Zaborac-Reed, 2019; Allen et al., 2020). Fossil flora indicates that vegetation surrounding the lake was mostly riparian hardwoods and tall Cupressaceae conifers with xeric chaparral flora and Pinaceae conifers at higher elevations (MacGinite, 1953; McLeroy and Anderson, 1966; Allen et al., 2020). Angiosperms are diverse and the dominant component of the flora, although the most common conifers include *Chamaecyparis*, *Sequoia* and less common Torreya, Abies, Picea, and Pinus (MacGinite, 1953; Manchester, 2001). Some of the most abundant angiosperms include Fagopsis, Cedrelospermum, and Sapindus, with a diversity of other angiosperms also preserved (Gregory, 1994; Allen et al., 2020).

246

247

248

249

250

251

252

253

231

232

233

234

235

236

237

238

239

240

241

242

243

244

245

## 2.2. Sample preparation and lipid extraction from sediments

Sediment-derived leaf wax n-alkanes (n-C<sub>27</sub> to n-C<sub>35</sub>) and di- and triterpenoids were targeted in this study. Sediment samples were powdered and lipids were extracted using an accelerated solvent extractor (Dionex ASE 350) with DCM/MeOH (5:1, v/v). From the total lipid extract (TLE), the asphaltenes were precipitated from the maltene fraction using DCM/hexanes (1:80, v/v). Using column chromatography, the maltene fraction was further divided into apolar and polar fractions on alumina oxide with hexanes/DCM (9:1, v/v) and

DCM/MeOH (1:1, v/v), respectively. The apolar fraction was separated into saturated and unsaturated fractions on 5% Ag<sup>+</sup>-impregnated silica gel (w/w) with hexanes and ethyl acetate, respectively. Methodology for the Bighorn Basin sediments is reported in Diefendorf et al. (2014; 2015a) and was very similar with the exception of analytical equipment that varied in model and vintage.

### 2.3. Compound identification and quantification

*n*-Alkanes were identified and quantified from the apolar, saturated fraction. Di- and triterpenoids were identified and quantified from the apolar, saturated, and unsaturated fractions. All samples were diluted in hexanes and injected into an Agilent 7890A gas chromatograph (GC) interfaced to an Agilent 5975C quadrupole mass selective detector (MSD) and flame ionization detector (FID). Compounds were separated on a fused silica capillary column (Agilent J&W DB-5ms; 30 m length, 0.25 mm i.d., 0.25 μm film thickness). The oven program started with an initial temperature of 60 °C for 1 min, followed by a 6 °C/min temperature ramp to 320 °C and held for 15 min. Following the GC separation, the column effluent was split (1:1) between the FID and MSD using a 2-way splitter, using He makeup gas to keep pressure constant. A scan range of *m*/*z* 45–700 at 2 scans/s was used, with an ionization energy of 70 eV. Compounds were identified using *n*-alkane standards (C<sub>7</sub> to C<sub>40</sub>; Supelco, Bellefonte, USA), fragmentation patterns, retention times, and published spectra (see Table 2 and References therein).

The *n*-alkanes and terpenoids were quantified by FID using normalizing compound peak areas relative to an internal standard (1,1'-binaphthalene for *n*-alkanes and  $5\alpha$ -cholestane for terpenoids) and converting normalized peak areas to mass using external standard response curves (also normalized to the internal standard). The external standard curves ranged in

concentration from 0.5 to 100  $\mu$ g/ml and included 1,1'-binaphthalene and 5 $\alpha$ -cholestane at the same concentration as the internal standard and a series of *n*-alkanes of varying chain length, from C<sub>7</sub> to C<sub>40</sub> (Supelco, Bellefonte, USA). Compound concentrations were then normalized to the dry sediment mass ( $\mu$ g/g).

Thermal maturity of the organic matter was assessed using the homohopane ( $C_{31}$ ) maturity index for the isomerism at C-22 (Peters et al., 2005). The 22S (biological) and 22R (geological) isomer abundances were measured from the  $17\alpha$ ,21 $\beta$ -homohopane using GC–MS and the m/z 191, 205, and 426 ions. Homohopane maturity indices were calculated using the 22S/(22S + 22R) ratio for each sample and verified on each ion to rule out interferences. Homohopane values > 0.55 indicate the beginning of the early oil window (Peters et al., 2005). For our study, average values for each region ranged from 0.01 from the Late Paleocene/Early Eocene Arctic coal swamp to 0.54 at Creede, indicating all samples are below this early oil window.

## 2.4. Bulk carbon analysis and Total Organic Carbon (TOC)

For bulk isotope analysis, an aliquot of each sample was decarbonated by exposing the sediment to 1 N HCl for 30 min or until the reaction was complete and then neutralized using DI water rinses. The  $\delta^{13}$ C of bulk organic carbon and weight percent of total organic carbon (wt% TOC) were determined via continuous flow (He; 120 ml/min) on a Costech elemental analyzer (EA) coupled to a Thermo Electron Delta V Advantage Isotope Ratio Mass Spectrometer (IRMS). The  $\delta^{13}$ C values were corrected for sample size dependency and normalized to the VPDB scale using a two-point calibration (e.g., Coplen et al., 2006). Additional independent standards were measured in all EA runs to determine error. Long term combined precision and

accuracy of all EA runs was 0.12% ( $1\sigma$ ; n=30) and -0.13% (n=30), respectively. Total organic carbon in samples ranged from 0.7% to 47%.

### 2.5. Compound-specific carbon isotope analyses

Prior to isotope analysis, samples with n- $C_{29}$  or n- $C_{31}$  alkanes that were coeluting with other compounds or that had complex baselines were additionally cleaned using urea adduction to separate n-alkyl compounds from branched and cyclic compounds. Branched/cyclic compounds were separated by adducting n-alkanes in urea crystals with equal parts of 10% urea in methanol (w/w), acetone, and n-pentane by freezing and subsequent evaporation with nitrogen. Non-adducts were extracted with hexanes, and urea crystals were subsequently dissolved with water and methanol to release n-alkanes and then liquid-liquid extracted with hexanes to recover the n-alkanes.

Compound-specific carbon isotope analyses were performed, where possible, on n-C<sub>27</sub> to n-C<sub>35</sub> alkanes, diterpenoids, and triterpenoids by GC-combustion-IRMS. The  $\delta^{13}$ C composition of these compounds could not be obtained for all samples due to low abundances, high backgrounds, or coelutions with other compounds. Terpenoid compounds used for carbon isotope analysis are listed in Table 2. GC-C-IRMS was performed using a Thermo Trace GC Ultra coupled to an Isolink combustion reactor (Ni, Cu, and Pt wires) and Thermo Electron Delta V Advantage IRMS. Isotopic abundances were normalized to the VPDB scale using Mix A6 and A7 (Arndt Schimmelmann, Indiana University). The pooled carbon isotope analytical uncertainty was measured across all sample runs with co-injected n-C<sub>41</sub> alkanes and was 0.6% ( $1\sigma$ , n = 100) following Polissar and d'Andrea (2014). Additionally, an in-house n-alkane standard prepared from oak leaves (Oak-1a) was analyzed every 5 or 6 runs with a combined precision and

accuracy of 0.2‰ ( $1\sigma$ ; n = 77) and 0.04‰ (n = 77). All statistical analyses were performed using JMP Pro 14.0.0 (SAS Institute Inc, Cary, NC, USA).

325

326

327

328

329

330

331

332

333

334

335

336

337

338

339

340

341

342

343

344

345

323

324

### 3. Results and Discussion

#### 3.1. Organic matter characterization

Individual sites from the Bighorn Basin and Arctic were grouped into regional localities based on similar paleobotanical assemblages, depositional environments, and ages (Table 1). Pristane (Pr) to phytane (Ph) ratios are used to characterized redox conditions of organic matter and terrestrial matter input in geologic sediments (Powell and McKirdy, 1973; Bustin, 1988; Bechtel et al., 2004). Uncertainty exists regarding the biological sources (plant vs bacterial) and thermal conditions under which pristane and phytane are produced (Goossen et al., 1984; Tissot and Welte, 1984; ten Haven et al., 1987), although in practice, Pr/Ph values < 1 are considered reducing environments and Pr/Ph values > 3 are considered oxidizing environments (Hughes et al., 1995; Peters et al., 2005). We found substantial variability in Pr/Ph ratios within depositional environments, indicating a wide range of redox conditions across terrestrial landscapes. Coal swamps and floodplain depositional environments have higher average Pr/Ph ratios (6.1 and 2.3, respectively) than lacustrine environments (1.1), indicating more oxic conditions and higher plant input. However, a t-test reveals only floodplain and lacustrine depositional environments are statistically unique (p < 0.0001), but sample coverage for coals is poor (n = 2) and floodplains show a large range in Pr/Ph ratios (0.01–12.5). When compared to the paleovegetation, samples from angiosperm-dominated sites have higher average Pr/Ph ratios (3.5) than sites with more

abundant conifers (1.2), a significant difference using a t-test (p < 0.0001; Fig. 2A). At least in

this study, conifers are more likely to be preserved in wet environments prone to anoxic conditions, and angiosperms tend to be better preserved in oxic environments, but more work needs to be done to rule out collection biases and limited sample coverage across some depositional environments. For instance, tocopherols are often linked to pristane formation and are especially common in coal swamp depositional environments, such that Pr/Ph ratios in these settings may be higher than expected (Goossens et al., 1984; Rybicki et al., 2020). However, conifers such as *Metasequoia*, *Taxodium*, and *Glyptostrobus* are commonly found in wet depositional environments (swamps), while angiosperms in general prefer better drained sites, as seen in other regions and times (Davies-Vollum and Wing, 1998).

3.2. The abundance of n-alkanes by chain length as a paleovegetation indicator

# 3.2.1. Carbon preference index

Carbon preference index (CPI) is used to determine odd chain length preference in long chain n-alkanes, where values > 1 signify higher odd over even n-alkane abundances (Marzi et al., 1993). Values > 1 are typical for leaf wax n-alkanes in sediments (Bray and Evans, 1961; Eglinton and Hamilton, 1967; Freeman and Pancost, 2013). Bush and McInerney (2013) showed that modern woody angiosperms have higher average CPI values than woody gymnosperms. However, there is considerable overlap in their CPI ranges, and woody plants, overall, demonstrate a large range in CPI values (> 1 to 100)( Diefendorf et al., 2011; Bush and McInerney, 2013). In this study, all samples have CPI values > 1. Sites with abundant conifers have both the highest and lowest CPI values, ranging from 1.2 to 6.5, whereas angiosperm sites have CPI values that range from 1.5 to 6.3 (Fig. 2B). While CPI values do vary by site, they are comparable to modern plant values. However, using a t-test (p < 0.6284), we find no apparent

distinction in CPI values between angiosperm-dominated paleobotanical sites vs conifer and mixed conifer sites.

## 3.2.2. Terrestrial to aquatic ratios

Terrestrial to aquatic ratios (TAR) have been used to differentiate aquatic (algal and/or bacterial) organic matter (short chain n-alkanes;  $C_{15}$  to  $C_{19}$ ) from higher plant organic matter (long chain n-alkanes;  $C_{27}$  to  $C_{31}$ ), with higher values indicating increased higher plant contributions to the sediment (Bourbonniere and Meyers, 1996; Meyers, 1997). TAR values in this study ranged from 0.11 at Creede to 193 from the Arctic coal swamp sample (Fig. 2C). We find low TAR (< 1) values correspond to the sites with higher amounts of conifers, with the exception of the Arctic coal swamp sample with the highest TAR (t-test; p < 0.0001). This suggests conifers are better preserved in depositional environments with higher aquatic/bacterial input compared to angiosperms, with the notable exception of the one Artic coal site. This site had high CPI values (6.2) and very low thermal maturity (0.01), suggesting that there was very little bacteria or aquatic input to make short chain n-alkanes. It is also possible that sites with abundant angiosperms are producing high amounts of long chain n-alkanes, leading to higher TAR values at angiosperm sites vs most conifer sites.

### 3.2.3. Average chain length

Average chain length (ACL) is commonly used to document the relative amounts of different plant wax *n*-alkane chain lengths (Freeman and Pancost, 2013). ACL has been used as a paleovegetation proxy, but shows varying degrees of sensitivity to phylogeny, climate, and

biome (Diefendorf and Freimuth, 2017). Average chain lengths were calculated using the modified equation:

394 ACL' = 
$$\frac{(27n-C_{27}+29n-C_{29}+31n-C_{31}+33n-C_{33}+35n-C_{35})}{(n-C_{27}+n-C_{29}+n-C_{31}+n-C_{33}+n-C_{35})}$$
 (1)

The equation was modified from Eglinton and Hamilton (1967) to exclude *n*-C<sub>25</sub> alkanes, whose source can often include submerged aquatic plants (Ficken et al., 2000; Freeman and Pancost, 2013; Diefendorf and Freimuth, 2017), but resulting values are similar. At our sites, ACL' values ranged from 27.5 at Creede to 31.3 at Florissant, falling within the range observed in modern tree species (26–34; Diefendorf et al., 2011). The range in ACL' values at our sites is likely sensitive to variations in plant communities (i.e., different representative phylogenies, water use efficiency strategies, deciduousness). However, there is no significant difference between sites with high and low conifer abundances (29.0 vs 29.4, Fig. 2D). Modern conifer ACL values have a strong phylogenetic signal among most conifer groups (Diefendorf et al., 2015b). However, the range in the Cupressaceae and Pinaceae ACL values, which are the most dominant conifers in this study, overlap with the ACL range for angiosperms. As a result, ACL likely has limited applications for distinguishing between angiosperm and conifer communities for many Paleogene sites in the Northern Hemisphere.

3.3. Relative abundances of terpenoids and n-alkanes as vegetation indicators

Di- and triterpenoids were present in all but a few samples. Across all sites, the most abundant diterpenoid groups included the abietanes and pimaranes, with lesser amounts of beyerenes, kauranes, phyllocladanes, and a labdane. The most abundant triterpenoids were a

suite of dinoroleanane compounds that were at times coeluting with an unknown pentacyclic triterpenoid, and also lesser amounts of des-A-lupanes. Long chain n-alkanes were present in all samples. The n-C<sub>29</sub> and n-C<sub>31</sub> alkanes were most abundant, followed by n-C<sub>27</sub> alkanes and minor amounts of n-C<sub>33</sub> and n-C<sub>35</sub> alkanes.

To compare distributions of plant biomarkers between sites, the concentration (μg/g) of diterpenoids, triterpenoids, and *n*-alkanes (C<sub>27</sub> to C<sub>35</sub>) were summed for each sample, converted to relative percent, and averaged for each regional locality (Fig. 3). This approach provides a qualitative comparison of paleovegetation. For instance, at angiosperm sites, *n*-alkanes are the dominant plant biomarker (78–99%) with significantly lesser amounts of triterpenoids (0.9–9%) and diterpenoids (0.2–12%). At sites with higher amounts of conifers, excluding coal swamps, *n*-alkanes still represent the highest percentage of plant biomarkers (43–79%), the percentage of triterpenoids remains similar to angiosperm sites (0.1–15.4%), but the amount of conifer-derived diterpenoids increases (13–45%). In coal swamps, diterpenoids are the dominant biomarker (95–96%), with small amounts of *n*-alkanes (4–5%), and trace amounts of triterpenoids (0.2–0.3%).

When comparing the relative percent of n-alkanes and terpenoids between angiosperm and conifer dominated sites, there appears to be some defining patterns that may be useful to qualitatively determine the source of n-alkanes. For instance, the relative percent of n-alkanes to terpenoids are higher at angiosperm sites (78.4–98.9%) compared to conifer sites (3.9–66.8%) (Fig. 3; t-test, p = 0.0343). We suggest 80% as a cutoff for angiosperm-dominated sites. For example, n-alkanes proportions greater than 80% are correlated with the angiosperm sites. Under 80%, conifers are likely contributing, at least in part, to sedimentary n-alkanes. For instance, the Driftwood Canyon lacustrine environment has a high relative n-alkane abundance of 79.1%, and

based on the  $\delta^{13}$ C<sub>leaf</sub> values for this site, the sediment *n*-alkanes come from a roughly equal mix of conifers and angiosperms.

436

437

438

439

440

441

442

443

444

445

446

447

448

449

450

451

452

453

454

455

456

457

458

We also observe that when conifers are dominant on the landscape, the relative percent of diterpenoids is higher (13.1–95.8%) compared to angiosperm sites (0.2–12.3%) and this could also help indicate if n-alkanes are potentially conifer-derived. At conifer-dominated sites, Cupressaceae and Pinaceae were the most abundant groups, which can produce high amounts of the longer chain n-alkane homologues  $C_{33}$  and  $C_{35}$  (Diefendorf et al., 2015b), but if these conifer groups also produce high amounts of diterpenoids, then in combination this results in lower relative abundances of *n*-alkanes than at angiosperm sites. In coal depositional environments, the signal is swamped by high concentrations of diterpenoids. It is possible that in these depositional environments, conifer resins — which contain high abundances of diterpenoid compounds may also be preserved as amber (fossil resin), which are often found in coals (Otto et al., 2005). This would result in a biomarker preservation bias. Because of the exceptional preservation of diterpenoids in swamps, one cannot assume that *n*-alkanes are exclusively conifer-derived. For example, in the Driftwood Canyon coal swamp, diterpenoids are the dominant biomarkers (95.8%), but  $\delta^{13}$ C<sub>leaf</sub> values indicate *n*-alkanes are sourced from a mix of both conifers and angiosperms.

The percentage of triterpenoid biomarkers stays relatively uniform across both angiosperm and conifer sites, and therefore the amount of these compounds may not be useful indicators for the source of *n*-alkanes. Triterpenoids make up the smallest percent of the total plant biomarkers in this study, even in the Bighorn Basin and at Florissant where angiosperms are the dominant vegetation. Across all sites, we find triterpenoid compounds were either aromatized or underwent A-ring degradation (*des*-A compounds), both of which are indicative of

degradation to more stable configurations (Trendel et al., 1989; Rullkötter et al., 1994). Angiosperm-derived triterpenoids are known to have poorer preservation potential than conifer diterpenoids (Diefendorf et al., 2014; Giri et al., 2015). Preservation among diterpenoids and triterpenoids are not uniform due to aromatization as well as degradation of primary polar compounds in diterpenoids (e.g., ferruginol, dehydroabietic acid) and triterpenoids (e.g., amyrin, oleanoic acid) (Simoneit, 1977; Simoneit et al., 1986; Otto and Simoneit, 2001). With careful consideration of diagenetic processes, the relative abundances of n-alkanes and diterpenoids could be a useful first approach to determine if conifers contributed n-alkanes to the sediment. However, this is not a quantitative approach for estimating the vegetation sources of n-alkanes, especially due to preservational and diagenetic biases in different depositional environments. Further lines of evidences are needed to quantify the amount of conifer contribution to sediment n-alkanes, how this may differ among chain lengths, and the effect on their  $\delta^{13}$ C values.

## 3.4. Carbon isotopes of n-alkanes and terpenoids

To compare the  $\delta^{13}$ C values of the measured n-alkanes, diterpenoids, and triterpenoids, the data were grouped to account for differences in the carbon isotopic composition of the atmospheric ( $\delta^{13}$ C<sub>atm</sub>) through time and for differences in biosynthetic fractionation ( $\epsilon$ ), (i.e., the difference between  $\delta^{13}$ C values of the leaf and plant lipid). Sites span most of the Paleogene from 63 Ma to 26.59 Ma. During this time,  $\delta^{13}$ C<sub>atm</sub> values fluctuated by 2–3‰, a signal preserved in the plant biomarkers (Tipple et al., 2011). To avoid issues with constraining the exact ages of all sites, which in some cases are known only within a few Myr (e.g., late Paleocene/early Eocene Arctic sites), the measured n-alkane, diterpenoid, and triterpenoid  $\delta^{13}$ C values from the same regions and times have been averaged together. To make each region directly comparable,  $\delta^{13}$ C

values of di- and triterpenoids and the long chain n-alkane homologues have been plotted relative to their respective n- $C_{29}$  alkane  $\delta^{13}C$  values (Fig. 4) to account for differences in biosynthetic carbon isotope fractionation. Whereas n-alkanes are synthesized via the acetogenic pathway, diterpenoids are synthesized by the 2-C-methyl-D-erythritol-4-phosphate (MEP) pathway, and triterpenoids are created via the mevalonic acid pathway (MVA). Each pathway has a unique  $\varepsilon$  value from bulk leaf tissue to lipid biomarker. So even though conifers create both n-alkanes and diterpenoids (and angiosperms create both n-alkanes and triterpenoids), each biomarker type will have unique  $\delta^{13}C$  values as a result of these differences in fractionation (i.e.  $\varepsilon$  values). The  $\delta^{13}C$  values of n-alkanes, di- and triterpenoids were also compared to those of modern angiosperms and conifers and were taken from (Diefendorf et al., 2012; 2015b; 2019; Diefendorf and Freimuth, 2017).

Modern conifer leaf  $\delta^{13}$ C values average 2–3‰ higher than angiosperms from the same location (Diefendorf et al., 2010) with similar offsets in the lipid values (Murray et al., 1998; Mckellar et al., 2011). For all samples in this study, averaged by location, we observe a 3.7 ± 1.5‰ ( $1\sigma$ , n = 30) difference between measured conifer-derived diterpenoids and angiospermderived triterpenoids  $\delta^{13}$ C values (t-test, p = 0.0048). This is good evidence that the physiological responses to the environment, such as differences in water-use efficiency, between conifers and angiosperms have been similar since at least the Paleogene. Because there is little difference in  $\epsilon$  values between diterpenoids and triterpenoids, direct comparisons can be made between these biomarkers and the *n*-alkane values (Diefendorf et al., 2012). The  $\delta^{13}$ C values for diterpenoids and triterpenoids can be used effectively as end members for conifer and angiosperm taxa in our samples to trace the vegetation source of *n*-alkanes. Samples from the Latest Paleocene site (Bighorn Basin, WY) were omitted because diterpenoid  $\delta^{13}$ C values were anomalously low in

comparison to the triterpenoids  $\delta^{13}C$  values in the same samples and when compared to diterpenoid  $\delta^{13}C$  values of similarly aged samples in the same basin.

For both modern angiosperms and geologic sites with abundant angiosperms, triterpenoids were on average ~4‰ higher than n- $C_{29}$  alkane values (Fig. 4). In modern angiosperms, the  $\delta^{13}$ C values of n-alkanes were similar across all chain lengths. Modern angiosperms reported in Diefendorf et al. (2012) do not include values for n- $C_{35}$  alkanes due to the low abundance of those chain lengths. In this study, the samples at angiosperm-dominated sites had relatively uniform n-alkane  $\delta^{13}$ C values. The exception is for the n- $C_{35}$  alkanes, which are 1.2‰ higher relative to the n- $C_{29}$  alkanes at the Bighorn Basin Paleocene location. This is likely attributed to some conifer contribution. At the paleobotanical angiosperm sites, where available, diterpenoid values averaged  $6.6 \pm 1.0$ ‰ ( $1\sigma$ , n = 22) higher than the n- $C_{29}$  alkanes (t-test, p < 0.0001).

Modern conifer diterpenoid  $\delta^{13}$ C values have a much broader range of values relative to  $n\text{-}C_{29}$  alkanes. For instance, the average  $\delta^{13}$ C diterpenoid values for the groups Pinaceae and Cupressaceae are 2.5% and 3% greater than  $n\text{-}C_{29}$  alkanes, respectively, although large standard deviations exist (t-test, p = 0.0022). Taxaceae samples have a 5.6% difference between diterpenoids and  $n\text{-}C_{29}$  alkanes, and while large standard deviations do exist, the low sample numbers (n = 2) preclude a t-test. Unlike modern angiosperms, the  $\delta^{13}$ C values of n-alkanes in modern Cupressaceae, Pinaceae, and Taxaceae increase relative to the  $n\text{-}C_{29}$  alkane with increasing chain length. At paleobotanical conifer sites, diterpenoid  $\delta^{13}$ C values are 4.6% higher than  $n\text{-}C_{29}$  alkane (t-test, p < 0.0001). During the Paleocene and early Eocene, both angiosperm and conifer sites had similar offsets between diterpenoid and  $n\text{-}C_{29}$  alkane  $\delta^{13}$ C values. However, during the middle Eocene and Oligocene, this offset diminishes. This may be the result of

increasing conifer contribution to the n-alkanes or differences in conifer palaeoflora communities, resulting in different  $\varepsilon$  values. For instance, deciduous conifers dominate the early Eocene Arctic and Driftwood sites (Eberle and Greenwood, 2012; Eberle et al., 2014; Greenwood et al., 2016). Macrofossil and pollen data indicate increasing abundance of evergreen conifers during the middle Eocene Arctic and exclusively evergreen conifers are present at the Oligocene Creede site (Wolfe and Schorn, 1989; McIver and Basinger, 1999). When present, the  $\delta^{13}$ C values of n-C<sub>33</sub> and n-C<sub>35</sub> alkanes increase relative to n-C<sub>29</sub> alkane at conifer sites, similarly to modern conifers. Of note, the offset between triterpenoids and the n-C<sub>29</sub> alkane is 0% at conifer sites, as compared to  $\sim$ 4% at angiosperm sites, which is compelling evidence that sediment n-alkanes being sourced from different taxa across angiosperm and conifer dominated paleobotanical sites.

3.5. Leaf carbon isotopes of n-alkanes and terpenoids

To further consider how the  $\delta^{13}$ C values of *n*-alkanes are influenced by conifers, the  $\delta^{13}$ C values of triterpenoids and diterpenoids were converted to bulk  $\delta^{13}$ C<sub>leaf</sub> values, thereby accounting for differences in biosynthetic fractionation ( $\varepsilon_{lipid-leaf}$ ) that occur during the synthesis of these different lipid biomarkers (Diefendorf et al., 2012).

$$\varepsilon_{\text{lipid-leaf}} = \left(\delta^{13} C_{\text{lipid-biomarker}} + 1\right) / \left(\delta^{13} C_{\text{leaf}} + 1\right) \tag{2}$$

The  $\delta^{13}C_{leaf}$  values derived from the triterpenoids and diterpenoids represent end member  $\delta^{13}C$  values of angiosperm and conifer leaves, respectively, from the sediment samples. The *n*-alkanes were also converted to  $\delta^{13}C_{leaf}$  values and, depending on the vegetation source, have

values that plot closer to conifer leaf values, angiosperm leaf values, or intermediately, indicating a mixed source. The  $\varepsilon_{\text{triterpenoid}}$  value used for angiosperms (-0.4%) was derived from a global compilation of modern woody angiosperm vegetation (Diefendorf et al., 2012). The \(\epsilon\_{\text{diterpenoid}}\) value for conifers (-0.75%) is an average of modern Cupressaceae, Pinaceae, and Taxaceae conifer families (Diefendorf et al., 2015b). The  $\varepsilon_{\text{diternenoid}}$  value used for Creede was -3.3%, and represents an averaged ε<sub>diterpenoid</sub> value for Pinaceae genera and the genus *Juniperus* (Diefendorf et al., 2015b, 2019). Creede represents a rarely preserved conifer community dominated by evergreen Juniperus (Cupressoideae) and Pinaceae species, which sets it apart from the other paleobotanical locations inhabited mostly by deciduous Cupressaceae and Taxaceae. Juniperus, which makes up roughly half of the specimen abundance at Creede, has a significantly more negative  $\varepsilon$  value (-7.1%) compared to other Cupressaceae (-1.1%), Taxaceae (-1.0%), and Pinaceae (0.57‰), likely resulting in the small offset between the diterpenoids and *n*-alkanes. This is important evidence that different taxa may affect  $\delta^{13}$ C values of *n*-alkanes, and careful consideration should be taken when working in geologic and modern sites where large vegetation fluctuations occur.

551

552

553

554

555

556

557

558

559

560

561

562

563

564

565

566

567

568

569

570

571

572

573

The  $\varepsilon_{n\text{-alkane}}$  values used in this study were derived from a global compilation of woody vegetation (Diefendorf and Freimuth, 2017) and represent an average of both angiosperm and conifer values. For  $n\text{-}C_{27}$ ,  $C_{29}$ ,  $C_{31}$ ,  $C_{33}$ ,  $C_{35}$  alkanes,  $\varepsilon_{n\text{-alkane}}$  values were –4.2%, –4.7%, –5.1%, –4.6%, –3.2%, respectively. The  $\delta^{13}C_{\text{leaf}}$  values for n-alkane were also separately calculated using  $\varepsilon_{n\text{-alkane}}$  values for angiosperms and conifers, resulting in only minor differences in  $\delta^{13}C_{\text{leaf}}$  values and these do not change the following results and interpretations. Therefore, the values reported in the following sections are based on the averaged angiosperm and conifer  $\varepsilon_{n\text{-alkane}}$  values.

3.5.1. Bighorn Basin and Florissant

For the Paleocene and Eocene Bighorn Basin and Florissant paleobotanical sites, the flora is dominated by angiosperms with respect to relative biomass. Similar to modern plants, the difference between calculated  $\delta^{13}C_{leaf}$  values for angiosperms (derived from triterpenoids) and conifers (derived from diterpenoids) was 1.9% in the Paleocene and Eocene Bighorn Basin sediments. Diterpenoids were not abundant enough in Florissant samples to calculate conifer  $\delta^{13}C_{leaf}$  values, so the conifer  $\delta^{13}C_{leaf}$  end member was estimated based on the offset between modern angiosperms and conifers (3%). For both Paleocene and Eocene Bighorn Basin samples,  $\delta^{13}C_{leaf}$  values calculated using n- $C_{27}$  to  $C_{35}$  alkanes fall within the range of angiosperm leaves (Fig. 5). For Florissant, the  $\delta^{13}C_{leaf}$  values calculated using n- $C_{27}$ ,  $C_{29}$ , and  $C_{31}$  alkanes also fall within the  $\delta^{13}C$  range of angiosperm leaves. However,  $\delta^{13}C_{leaf}$  values calculated from n- $C_{33}$  alkanes show higher  $\delta^{13}C$  values, plotting closer to estimated conifer leaves, indicating a different vegetation source for these longer chain n-alkanes.

*3.5.2. Arctic* 

The Paleogene Arctic represents a mosaic of landscapes with abundant deciduous conifers flourishing in lowland swamps and poorly drained zones of floodplains, and diverse angiosperms at drier sites (Greenwood and Basinger 1994; McIver and Basinger 1999; West et al., 2019). The difference between angiosperms and conifer  $\delta^{13}C_{leaf}$  end members was -4.2% during the late Paleocene/early Eocene and -3.2% from the middle Eocene. For the late Paleocene/early Eocene Arctic floodplain samples,  $\delta^{13}C_{leaf}$  values increase with increasing chain length, indicating an increased conifer input, where the n- $C_{27}$  alkane show a fairly mixed

angiosperm-conifer source, and *n*-C<sub>33</sub> and *n*-C<sub>35</sub> alkanes have values that are consistent with being exclusively conifer-derived. Angiosperm-sourced outliers exist for each chain length. These samples are from Stenkul Fiord and coincide with vegetation-censused sites that were dominated by angiosperms and highlights the heterogeneity of vegetation across the Arctic landscape (West et al., 2019 and unpublished data).

The same comparison was done with the coal sample from Stenkul Fiord to investigate whether n-alkanes from different depositional environments (i.e., coal swamps vs floodplains) had similar vegetation sources. No triterpenoids were preserved in this coal sample, so angiosperm  $\delta^{13}C_{leaf}$  values were estimated based on the values at the other similarly aged Arctic sites. The  $\delta^{13}C_{leaf}$  values calculated from n- $C_{27}$  and  $C_{29}$  alkanes plot much closer to angiosperm leaves, whereas the  $\delta^{13}C_{leaf}$  values calculated from n- $C_{31}$ ,  $C_{33}$ , and  $C_{35}$  alkanes indicate a conifer source.

For the middle Eocene Arctic floodplain,  $\delta^{13}C_{leaf}$  values derived from n- $C_{27}$  to  $C_{35}$  alkanes all appear to be conifer-derived. This may indicate an increase in conifer abundance on the regional landscape, or perhaps because of limited sample size, may represent only a localized patch of conifer-dominated vegetation. Regardless, conifers appear to be the main contributor of n-alkanes across different depositional environments and time periods in the Paleogene Arctic, especially the longer chain lengths (n- $C_{33}$  and n- $C_{35}$ ).

### 3.5.3. Driftwood Canyon

Samples from the early Eocene Driftwood Canyon in British Columbia were grouped by depositional environment to explore the possible differences in the source of *n*-alkanes between a lacustrine and swamp setting, both of which are more representative of in situ vegetation regimes

than floodplain environments (Greenwood and Basinger, 1994; Freimuth et al., 2019). The difference between angiosperms and conifer  $\delta^{13}C_{leaf}$  end members was –6‰ in the coal swamp depositional environment. Triterpenoids were not measurable in the lacustrine sediments, so angiosperm end members were estimated at ~6‰ lower than conifers. In lacustrine sediments, the  $\delta^{13}C_{leaf}$  values calculated using n- $C_{27}$  to n- $C_{35}$  alkanes fall between the angiosperm and conifer  $\delta^{13}C_{leaf}$  end members, indicating a mixed vegetation source. However, as in the Arctic region, longer chain n-alkanes show incrementally higher values, indicating more conifer input. In the coal swamp samples, the  $\delta^{13}C_{leaf}$  values calculated using n- $C_{27}$ ,  $C_{29}$ ,  $C_{31}$ , and  $C_{33}$  alkanes also indicate a mixed angiosperm-conifer source and did not show much variability between the chain lengths.

### 3.5.4. Creede

Only trace amounts of triterpenoids were detected in the Creede samples; therefore, angiosperm  $\delta^{13}C_{leaf}$  end members were estimated to be 3% lower than the  $\delta^{13}C_{leaf}$  values of the conifers. The lack of triterpenoids is not unexpected because macrofossils indicate that this site was dominated by *Juniperus* and Pinaceae. The  $\delta^{13}C_{leaf}$  values calculated using n- $C_{27}$ ,  $C_{29}$ ,  $C_{31}$ , and  $C_{33}$  alkanes fell within the range of conifer  $\delta^{13}C_{leaf}$  values. The  $\delta^{13}C_{leaf}$  value derived from the n- $C_{35}$  alkane was more negative than the other chain lengths and could indicate a different vegetation source or possibly some uncertainty associated with the estimated  $\varepsilon_{n$ -alkane value.

3.6. Determining vegetation source of n-alkanes in geologic sediments from terpenoid  $\delta^{13}C$  values and isotopic mixing models

To further evaluate the efficacy of using terpenoid  $\delta^{13}$ C values as vegetation end members to determine the source of sediment n-alkanes, the calculated  $\delta^{13}$ C<sub>leaf</sub> values of n-alkanes, diterpenoids, and triterpenoids were used in an isotope mass-balance equation to estimate the percent of conifer contribution to the different long chain n-alkanes at each region:

Conifer (%) =  $(\delta^{13}C_{\text{leaf-alkane}} - \delta^{13}C_{\text{angiosperm leaf}}) / (\delta^{13}C_{\text{conifer leaf}} - \delta^{13}C_{\text{angiosperm leaf}}) \times 100$  (3)

where  $\delta^{13}C_{\text{leaf-alkane}}$  is the mean bulk leaf  $\delta^{13}C$  value derived from the *n*-alkanes, and the  $\delta^{13}C_{\text{angiosperm leaf}}$  and  $\delta^{13}C_{\text{conifer leaf}}$  are the mean bulk leaf  $\delta^{13}C$  values derived from triterpenoids and diterpenoids, respectively.

The values from the mixing model are shown in Table 3. A Monte Carlo simulation method was performed to quantify Gaussian uncertainty ( $1\sigma$ ) in  $\Delta_{leaf}$  values for each site using 10,000 iterations in MATLAB R2017a (The MathWorks, Natick, USA). Input uncertainties included the standard deviations of  $\delta^{13}C_{leaf-alkane}$ ,  $\delta^{13}C_{conifer\ leaf}$  and  $\delta^{13}C_{angiosperm\ leaf}$  for each region. Uncertainties for  $\epsilon$  values were omitted based on studies that suggest modern calibrations overestimate error because modern ranges in variability are much higher than would be expected in geologic sediment, which represents many integrated plants through time (Polissar et al., 2009; Diefendorf and Freimuth, 2017).

Previous work highlighted that conifers could contribute *n*-alkanes to the sediment and affect carbon isotope values (Smith et al., 2008; Diefendorf et al., 2011; 2014; 2015). These studies estimated the percent of conifer macroflora in the Paleocene and Eocene Bighorn Basin at between 13–14% (Smith et al., 2008) and 1–34% (Diefendorf et al., 2014), but did not have a mechanism to estimate how much conifers were contributing to the sediment *n*-alkanes or

quantify how this would affect their  $\delta^{13}$ C values. Here we provide a method to test the vegetation source of *n*-alkanes during the Paleogene by using the  $\delta^{13}$ C values of diterpenoids and triterpenoids to calculate conifer and angiosperm  $\delta^{13}C_{leaf}$  values to serve as taxonomic end members for each location (Fig. 5). We suggest calling this approach the *terpenoid-isotope* taxonomic estimator (TITE). As part of TITE, we used the  $\delta^{13}C_{leaf}$  end member values to run isotopic mixing models to estimate conifer contribution by n-alkane chain length. For the n-C<sub>29</sub> alkane in the Bighorn Basin, we find that conifers contribute 0–16% of the *n*-alkanes, which agrees well with estimates of the macroflora assemblages (Smith et al., 2012; Diefendorf et al., 2014). This method goes one step further to assess how conifer contribution affects  $\delta^{13}$ C of nalkanes. At angiosperm sites in the Bighorn Basin, the minor amount of conifer contribution has little effect on the overall  $\delta^{13}$ C values of *n*-alkanes (Fig. 5). However, at Florissant, the isotopic mixing model shows conifers are contributing  $\sim 16 \pm 30\%$  (1 $\sigma$ , n = 17) to the *n*-C<sub>33</sub> homologue, which produces a small positive shift in the  $\delta^{13}C_{leaf}$  values (Fig. 5). These results suggest that even at angiosperm-dominated sites, conifers contribute some minor amount of longer chain nalkanes to the sediment and, in some cases,  $\delta^{13}$ C values of the longer chain homologues may be increasingly sensitive to different vegetation sources.

665

666

667

668

669

670

671

672

673

674

675

676

677

678

679

680

681

682

683

684

685

686

In mixed conifer environments, such as Driftwood Canyon, about half of the n-alkanes are sourced from conifers (Table 3). As a result,  $\delta^{13}$ C values of n-alkanes are  $\sim$ 2–4‰ higher for all C<sub>27</sub> to C<sub>35</sub> chain lengths than would be expected from a purely angiosperm source (Fig. 5). We also find that conifer input generally increases with longer chain n-alkanes at mixed conifer sites, affecting the  $\delta^{13}$ C values of C<sub>33</sub> and C<sub>35</sub> alkanes, while n-C<sub>27</sub> alkanes have the highest angiosperm input. This indicates that even when conifers contribute only partly to the sediment

n-alkanes, they can still have an important isotopic effect on the sedimentary n-alkane  $\delta^{13}$ C values (Fig. 5).

At some of the conifer-dominated sites (middle Eocene Arctic and Creede), 100% of n-alkanes (all chain lengths) are sourced from conifers. At other conifer sites, such as the late Paleocene/early Eocene Arctic, the n-C<sub>27</sub> alkanes have a significant amount of angiosperm contribution that ranges from 41% to 45% (Table 3) and conifer contribution increases with increasing n-alkane chain length. However, some sites show that the n-C<sub>35</sub> alkane has less conifer input than the n-C<sub>33</sub> alkane. It is likely that the  $\epsilon$  value for the n-C<sub>35</sub> homologue is not entirely accurate based on the sparse number of measurements in the modern calibration (Diefendorf and Freimuth, 2017) and could benefit from future studies on modern  $\epsilon$  calibrations.

#### 4. Conclusions

Long chain *n*-alkanes extracted from geologic sediment are not necessarily diagnostic of their vegetation source, as they are produced by both angiosperms and conifers. It is generally accepted that angiosperms produce high abundances of *n*-alkanes and thus can dominate the sediment distributions (Diefendorf et al., 2011, 2014; Bush and McInerney, 2013). While some conifer groups that were common in North America during earlier parts of the Paleogene, such as the Taxodioideae, or throughout the Cenozoic, such as the Pinaceae, tend to make low concentrations of *n*-alkanes, some conifers from groups such as the Cupressoideae and Callitroideae (Cupressaceae) produce significant amounts of *n*-alkanes (e.g., *Juniperus*), especially the longer chain lengths (*n*-C<sub>33</sub> and *n*-C<sub>35</sub>). This could be further tested at Triassic and Jurassic sites where *n*-alkanes are exclusively conifer-derived, prior to the evolution of angiosperms. In the Paleogene, though, not much is understood about the source of sediment *n*-

alkanes when these groups of conifers are the most abundant taxa on the landscape, or how this would impact their  $\delta^{13}$ C and  $\delta^{2}$ H isotopes, which has important consequences for the wide array of paleo proxies that use leaf wax n-alkanes. Understanding the paleovegetation source of n-alkanes may be especially important during times of rapid climate change, where leaf wax  $\delta^{2}$ H and  $\delta^{13}$ C values can reflect a complex signal of rapidly changing plant communities and climate.

We have provided a method to test the vegetation source of n-alkanes during the Paleogene by using  $\delta^{13}$ C values of terpenoids as conifer and angiosperm end members. We suggest calling this approach the *terpenoid-isotope taxonomic estimator* (TITE). Using this method, we find that n-alkanes can be exclusively or mostly derived from conifer sources when conifers are the dominant taxa on the landscape. We also find at conifer and mixed conifer sites that conifer contributions increase with increasing n-alkane chain length. At sites where angiosperms are the most abundant taxa, conifers can contribute some minor amount of n-alkanes, typically the n-C<sub>33</sub> and n-C<sub>35</sub> homologues, suggesting that conifers in the Paleogene contributed to longer chain n-alkanes (n-C<sub>33</sub> and n-C<sub>35</sub>) even when not the dominant taxa, but this likely differs for other geographic locations and taxa.

The approach presented here determines if n-alkanes are sourced from conifers and shows that it may be critical to measure all chain lengths ( $C_{27}$  to  $C_{35}$ ), but it also highlights that constraining the conifer taxa at a given site is important because different taxa have unique chain length and  $\varepsilon$  values. These will vary among different conifer taxa, especially Cupressaceae, Pinaceae, and Podocarpaceae. This approach may be useful for determining the source of n-alkane contributions when other taxonomic information (e.g., fossils or pollen) are not preserved, and has wider applications for regions outside of North American where different conifer assemblages were common, for other times in the past when conifers were common on the

landscape, and during periods of rapid climate change associated with large vegetation shifts (i.e., PETM; Smith et al., 2007).

735

736

737

740

741

744

745

746

733

734

# Acknowledgements

We thank Jeff Hannon for thoughtful discussions, Megan Brennan for assistance with sample 738 preparation, Sarah Hammer for laboratory management, and two anonymous reviewers for their helpful comments and suggestions. We also thank Talia Karim at the Colorado 739 University Museum of Natural History and Conni O'Connor at Florissant Fossil Beds National Monument for assistance with museum specimen sample collection. This research was supported by the U.S. National Science Foundation (EAR-1636546 to AFD), the Natural Sciences and 742 743 Engineering Research Council (NSERC) of Canada (Discovery grants to JFB 1334 and DRG 2016 - 04337), and the Polar Continental Shelf Project of Natural Resources Canada (to JFB). This research was supported by an NSERC Alexander Graham Bell Doctoral Scholarship (to CKW), and a Northern Scientific Training Program grant for conducting fieldwork in the Arctic 747 (to CKW). CKW acknowledges the assistance of various field party members in the collection of samples Stenkul Fiord on Ellesmere Island, and thanks Lutz Reinhardt and Karsten Piepjohn of 748 749 the Bundesanstalt für Geowissenschaften und Rohstoffe (BGR) [Federal Institute for Geosciences and Natural Resources] for funding and logistics in support of field work on Ellesmere Island. This research was also supported by awards from the University of Cincinnati 752 chapter of Sigma Xi and the Paleontological Society to KMS.

753

754

750

751

### Appendix A. Supplementary material.

- 755 Supplementary data associated with this article can be found at PANGAEA,
- 756 https://doi.org/10.1594/PANGAEA.919135.

757

758 Associate Editor-Klaas Nierop

759

- 760 References
- Allen, S.E., Lowe, A.J., Peppe, D.J., Meyer, H.W., 2020. Paleoclimate and paleoecology of the
- latest Eocene Florissant flora (Central Colorado, USA). Palaeogeography, Palaeoclimatology,
- 763 Palaeoecology 551, 109678.
- Baczynski, A.A., McInerney, F.A., Wing, S.L., Kraus, M.J., Bloch, J.I., Secord, R., 2017.
- Constraining paleohydrologic change during the Paleocene-Eocene Thermal Maximum in the
- continental interior of North America. Palaeogeography, Palaeoclimatology, Palaeoecology
- 767 465, 237–246.
- Barton, M.A., 2010. Floral diversity and climate change in central Colorado during the Eocene
- and Oligocene. Masters Thesis. University of Colorado, Boulder, Colorado, USA.
- Bechtel, A., Markic, M., Sachsenhofer, R.F., Jelen, B., Gratzer, R., Lücke, A., Püttmann, W.,
- 771 2004. Paleoenvironment of the upper Oligocene Trbovlje coal seam (Slovenia). International
- Journal of Coal Geology 57, 23–48.
- Bourbonniere, R.A., Meyers, P.A., 1996. Sedimentary geolipid records of historical changes in
- the watersheds and productivities of Lakes Ontario and Erie. Limnology and Oceanography
- 775 41, 352–359.
- Bray, E.E., Evans, E.D., 1961. Distribution of *n*-paraffins as a clue to recognition of source beds.
- Geochimica et Cosmochimica Acta 22, 2–15.

- Brooks, J.R., Flanagan, L.B., Buchmann, N., Ehleringer, J.R., 1997. Carbon isotope composition
- of boreal plants: Functional grouping of life forms. Oecologia 110, 301–311.
- Burke, K.D., Williams, J.W., Chandler, M.A., Haywood, A.M., Lunt, D.J., Otto-Bliesner, B.L.,
- 781 2018. Pliocene and Eocene provide best analogs for near-future climates. Proceedings of the
- National Academy of Sciences of the United States of America 115, 13288–13293.
- Bush, R.T., McInerney, F.A., 2013. Leaf wax *n*-alkane distributions in and across modern plants:
- Implications for paleoecology and chemotaxonomy. Geochimica et Cosmochimica Acta 117,
- 785 161–179.
- Bush, R.T., Wallace, J., Currano, E.D., Jacobs, B.F., McInerney, F.A., Dunn, R.E., Tabor, N.J.,
- 787 2017. Cell anatomy and leaf  $\delta^{13}$ C as proxies for shading and canopy structure in a Miocene
- forest from Ethiopia. Palaeogeography, Palaeoclimatology, Palaeoecology 485, 593–604.
- Buskirk, B.L., Bourgeois, J., Meyer, H.W., Nesbitt, E.A., 2016. Freshwater molluscan fauna
- from the Florissant Formation, Colorado: Paleohydrologic reconstruction of a latest Eocene
- lake. Canadian Journal of Earth Sciences 53, 630–643.
- Bustin, R.M., 1988. Sedimentology and characteristics of dispersed organic matter in Tertiary
- Niger Delta: origin of source rocks in a deltaic environment. American Association of
- 794 Petroleum Geologists Bulletin 72, 277–298.
- 795 Castañeda, I.S., Schouten, S., 2011. A review of molecular organic proxies for examining
- modern and ancient lacustrine environments. Quaternary Science Reviews 30, 2851–2891.
- 797 Chaffee, A.L., Fookes, C.J.R., 1988. Polycyclic aromatic hydrocarbons in Australian coals-III.
- 798 Structural elucidation by proton nuclear magnetic resonance spectroscopy. Organic
- 799 Geochemistry 12, 261–271.
- 800 Chaffee, A.L., Strachan, M.G., Johns, R.B., 1984. Polycyclic aromatic hydrocarbons in

- Australian coals. I. Novel tetracyclic components from Victorian brown coal. Geochimica et
- 802 Cosmochimica Acta 46, 2037–2043.
- 803 Chang, H.C.K., Nishioka, M., Bartle, K.D., Wise, S.A., Bayona, J.M., Markides, K.E., Lee,
- M.L., 1988. Identification and comparison of low-molecular-weight neutral constituents in
- two different coal extracts. Fuel 67, 45–57.
- 806 Coplen, T.B., Brand, W.A., Gehre, M., Gröning, M., Meijer, H.A., Toman, B., Verkouteren,
- 807 R.M., 2006. New guidelines for  $\delta^{13}$ C measurements. Analytical Chemistry 78, 2439–2441.
- 808 Currano, E.D., 2009. Patchiness and long-term change in early Eocene insect feeding damage.
- 809 Paleobiology 35, 484–498.
- 810 Currano, E.D., Wilf, P., Wing, S.L., Labandeira, C.C., Lovelock, E.C., Royer, D.L., 2008.
- Sharply increased insect herbivory during the Paleocene-Eocene Thermal Maximum.
- Proceedings of the National Academy of Sciences of the United States of America 105, 1960–
- 813 1964.
- 814 Czechowski, F., Stolarski, M., Simoneit, B.R.T., 2002. Supercritical fluid extracts from brown
- coal lithotypes and their group components molecular composition of non-polar
- compounds. Fuel 81, 1933–1944.
- Davies-Vollum, K.S., Wing, S.L., 1998. Sedimentological, taphonomic, and climatic aspects of
- Eocene swamp deposits (Willwood Formation, Bighorn Basin, Wyoming). Palaios 13, 28–40.
- Demetzos, C., Kolocouris, A., Anastasaki, T., 2002. A simple and rapid method for the
- differentiation of C-13 manoyl oxide epimers in biologically important samples using GC-MS
- analysis supported with NMR spectroscopy and computational chemistry results. Bioorganic
- and Medicinal Chemistry Letters 12, 3605–3609.
- Diefendorf, A.F., Freimuth, E.J., 2017. Extracting the most from terrestrial plant-derived *n*-alkyl

- lipids and their carbon isotopes from the sedimentary record: A review. Organic
- 825 Geochemistry 103, 1–21.
- Diefendorf, A.F., Freeman, K.H., Wing, S.L., 2012. Distribution and carbon isotope patterns of
- diterpenoids and triterpenoids in modern temperate C<sub>3</sub> trees and their geochemical
- significance. Geochimica et Cosmochimica Acta 85, 342–356.
- Diefendorf, A.F., Freeman, K.H., Wing, S.L., 2014. A comparison of terpenoid and leaf fossil
- vegetation proxies in Paleocene and Eocene Bighorn Basin sediments. Organic Geochemistry
- 831 71, 30–42.
- Diefendorf, A.F., Leslie, A.B., Wing, S.L., 2015b. Leaf wax composition and carbon isotopes
- vary among major conifer groups. Geochimica et Cosmochimica Acta 170, 145–156.
- Diefendorf, A.F., Leslie, A.B., Wing, S.L., 2019. A phylogenetic analysis of conifer diterpenoids
- and their carbon isotopes for chemotaxonomic applications. Organic Geochemistry 127, 50–
- 836 58.
- Diefendorf, A.F., Mueller, K.E., Wing, S.L., Koch, P.L., Freeman, K.H., 2010. Global patterns in
- leaf <sup>13</sup>C discrimination and implications for studies of past and future climate. Proceedings of
- the National Academy of Sciences of the United States of America 107, 5738–5743.
- Diefendorf, A.F., Freeman, K.H., Wing, S.L., Graham, H. V., 2011. Production of *n*-alkyl lipids
- in living plants and implications for the geologic past. Geochimica et Cosmochimica Acta 75,
- 842 7472–7485.
- Diefendorf, A.F., Freeman, K.H., Wing, S.L., Currano, E.D., Mueller, K.E., 2015a. Paleogene
- plants fractionated carbon isotopes similar to modern plants. Earth and Planetary Science
- 845 Letters 429, 33–44.
- Eberle, J.J., Fricke, H.C., Humphrey, J.D., Hackett, L., Newbrey, M.G., Hutchison, J.H., 2010.

- Seasonal variability in Arctic temperatures during early Eocene time. Earth and Planetary
- 848 Science Letters 296, 481–486.
- 849 Eberle, J.J., Greenwood, D.R., 2012. Life at the top of the greenhouse Eocene world A review
- of the Eocene flora and vertebrate fauna from Canada's High Arctic. Bulletin of the
- Geological Society of America 124, 3–23.
- 852 Eberle, J.J., Rybczynski, N., Greenwood, D.R., Taylor, P, 2014. Early Eocene mammals from
- the Driftwood Creek beds, Driftwood Canyon Provincial Park, northern British Columbia.
- Journal of Vertebrate Paleontology 34, 739–746.
- Eglinton, G., Hamilton, R.J., 1967. Leaf epicuticular waxes. Science 156, 1322–1335.
- Feakins, S.J., Wu, M.S., Ponton, C., Galy, V., West, A.J., 2018. Dual isotope evidence for
- sedimentary integration of plant wax biomarkers across an Andes-Amazon elevation transect.
- Geochimica et Cosmochimica Acta 242, 64–81.
- Ficken, K.J., Li, B., Swain, D.L., Eglinton, G., 2000. An *n*-alkane proxy for the sedimentary
- input of submerged/floating freshwater aquatic macrophytes. Organic Geochemistry 31, 745–
- 861 749.
- Freeman, K.H., Boreham, C.J., Summons, R.E., Hayes, J.M., 1994. The effect of aromatization
- on the isotopic compositions of hydrocarbons during early diagenesis. Organic Geochemistry
- 864 21, 1037–1049.
- Freeman, K.H., Pancost, R.D., 2013. Biomarkers for terrestrial plants and climate. In: Treatise on
- Geochemistry, Second Edition, Vol. 12. Elsevier, pp. 395–416
- Freimuth, E.J., Diefendorf, A.F., Lowell, T. V., Wiles, G.C., 2019. Sedimentary *n*-alkanes and *n*-
- alkanoic acids in a temperate bog are biased toward woody plants. Organic Geochemistry
- 869 128, 94–107.

- Garcin, Y., Schefuß, E., Schwab, V.F., Garreta, V., Gleixner, G., Vincens, A., Todou, G., Séné,
- O., Onana, J.M., Achoundong, G., Sachse, D., 2014. Reconstructing C<sub>3</sub> and C<sub>4</sub> vegetation
- cover using *n*-alkane carbon isotope ratios in recent lake sediments from Cameroon, Western
- 873 Central Africa. Geochimica et Cosmochimica Acta 142, 482–500.
- 674 Giri, S.J., Diefendorf, A.F., Lowell, T.V., 2015. Origin and sedimentary fate of plant-derived
- terpenoids in a small river catchment and implications for terpenoids as quantitative
- paleovegetation proxies. Organic Geochemistry 82, 22–32.
- Goossens, H.D., de Leeuw, J.W., Schenck, P.A., Brassell, S.C., 1984. Tocopherols as likely
- precursors of pristane in ancient sediments and crude oils. Nature 312, 440–442.
- Greenwood, D.R., Archibald, S.B., Mathewes, R.W., Moss, P.T., 2005. Fossil biotas from the
- Okanagan Highlands, southern British Columbia and northeastern Washington State:
- Climates and ecosystems across an Eocene landscape. Canadian Journal of Earth Sciences 42,
- 882 167–185.
- 683 Greenwood, D.R., Basinger, J.F., 1994. The paleoecology of high-latitude Eocene swamp forests
- from Axel Heiberg Island, Canadian High Arctic. Review of Palaeobotany and Palynology
- 885 81, 83–97.
- 686 Greenwood, D.R., Basinger, J.F., Smith, R.Y., 2010. How wet was the Arctic Eocene rain forest?
- Estimates of precipitation from Paleogene Arctic macrofloras. Geology 38, 15–18.
- 688 Greenwood, D.R., Pigg, K.B., Basinger, J.F., DeVore, M.L., 2016. A review of paleobotanical
- studies of the Early Eocene Okanagan (Okanogan) Highlands floras of British Columbia,
- Canada, and Washington, USA. Canadian Journal of Earth Sciences 53, 548–564.
- 6891 Gregory, K.M., 1994. Palaeoclimate and palaeoelevation of the 35 Ma Florissant flora, Front
- Range, Colorado. Palaeoclimates 1, 23–57.

- Harrington, G.J., Eberle, J., Le-page, B.A., Dawson, M., Hutchison, J.H., 2012. Arctic plant
- diversity in the Early Eocene greenhouse. Proceedings of the Royal Society B 279, 1515–
- 895 1521.
- Hickey, L.J., 1980. Paleocene stratigraphy and flora of the Clark's Fork Basin. In: Gingerich,
- P.D. (Ed.), Early Cenozoic Paleontology and Stratigraphy of the Bighorn Basin, Wyoming.
- University of Michigan Papers on Paleotology, pp. 295–311.
- Hren, M.T., Pagani, M., Erwin, D.M., Brandon, M., 2010. Biomarker reconstruction of the early
- Eocene paleotopography and paleoclimate of the northern Sierra Nevada. Geology 38, 7–10.
- Hughes, W.B., Holba, A.G., Dzou, L.I.P., 1995. The ratios of dibenzothiophene to phenanthrene
- and pristane to phytane as indicators of depositional environment and lithology of petroleum
- source rocks. Geochimica et Cosmochimica Acta 59, 3581–3598.
- Jacob, J., Disnar, J.R., Boussafir, M., Spadano Albuquerque, A.L., Sifeddine, A., Turcq, B.,
- 2007. Contrasted distributions of triterpene derivatives in the sediments of Lake Caçó reflect
- paleoenvironmental changes during the last 20,000 yrs in NE Brazil. Organic Geochemistry
- 907 38, 180–197.
- Killops, S., Raine, J.I., Woolhouse, A.D., Weston, R.J., 1995. Chemostratigraphic evidence of
- higher-plant evolution in the Taranaki Basin, New Zealand. Organic Geochemistry 23, 429–
- 910 445.
- Lane, C.S., 2017. Modern *n*-alkane abundances and isotopic composition of vegetation in a
- 912 gymnosperm-dominated ecosystem of the southeastern U.S. coastal plain. Organic
- 913 Geochemistry 105, 33–36.
- Lane, C.S., Taylor, A.K., Spencer, J., Jones, K.B., 2018. Compound-specific isotope records of
- late-quaternary environmental change in southeastern North Carolina. Quaternary Science

- 916 Reviews 182, 48–64.
- Larsen, D., Crossey, L.J., 1996. Depositional environments and paleolimnology of an ancient
- caldera lake: Oligocene Creede Formation, Colorado. Geological Society of America Bulletin
- 919 108, 526–544.
- Leonardi, S., Gentilesca, T., Guerrieri, R., Ripullone, F., Magnani, F., Mencuccini, M., Noije, T.
- V., Borghetti, M., 2012. Assessing the effects of nitrogen deposition and climate on carbon
- isotope discrimination and intrinsic water-use efficiency of angiosperm and conifer trees
- under rising CO<sub>2</sub> conditions. Global Change Biology 18, 2925–2944.
- Leopold, E.B., Clay-Poole, S.T., 2001. Florissant leaf and pollen floras of Colorado compared:
- climatic implications. In: Fossil Flora and Stratigraphy of the Florissant Formation, Colorado.
- Proceedings of the Denver Museum of Nature and Science, pp. 17–70.
- Leopold, E.B., Zaborac-Reed, S., 2014. Biogeographic history of *Abies bracteata* (D. Don) A.
- Poit. in the Western United States. In: Stevens, W.D., Montiel, O.M., Raven, P.H. (Eds).
- Paleobotany and Biogeography. Missouri Botanical Garden Press, St Louis, pp. 252–286.
- Leopold, E.B., Zaborac-Reed, S., 2019. Pollen evidence of floristic turnover forced by cool
- aridity during the Oligocene in Colorado. Geosphere 15, 254-294.
- Leslie, A.B., Beaulieu, J.M., Rai, H.S., Crane, P.R., Donoghue, M.J., Mathews, S., 2012.
- Hemisphere-scale differences in conifer evolutionary dynamics. Proceedings of the National
- Academy of Sciences of the United States of America 109, 16217–16221.
- 935 MacGinitie, H.D., 1953. Fossil Plants of the Florissant Beds, Colorado. Carnegie Institution of
- Washington Publication 599, Washington DC, USA.
- 937 MacIntyre, D.G., Villeneuve, M.E., Schiarizza, P., 2001. Timing and tectonic setting of Stikine
- 938 Terrane magmatism, Babine-Takla lakes area, Central British Columbia. Canadian Journal of

- 939 Earth Sciences 38, 579–600.
- Magill, C.R., Ashley, G.M., Freeman, K.H., 2013. Ecosystem variability and early human
- habitats in eastern Africa. Proceedings of the National Academy of Sciences 110, 1167–1174.
- Manchester, S.R., 2001. Update on the megafossil flora of Florissant, Colorado. In: Fossil Flora
- and Stratigraphy of the Florissant Formation, Colorado. Proceedings of the Denver Museum
- of Nature and Science, pp. 137–162.
- 945 Marzi, R., Torkelson, B.E., Olson, R.K., 1993. A revised carbon preference index. Organic
- 946 Geochemistry 20, 1303–1306.
- McIver, E.E., Basinger, J.F., 1999. Early Tertiary floral evolution in the Canadian High Arctic.
- Annals of the Missouri Botanical Garden 86, 523–545.
- 949 Mckellar, R.C., Wolfe, A.P., Muehlenbachs, K., Tappert, R., Engel, M.S., Cheng, T., Sánchez-
- Azofeifa, G.A., 2011. Insect outbreaks produce distinctive carbon isotope signatures in
- defensive resins and fossiliferous ambers. Proceedings of the Royal Society B: Biological
- 952 Sciences 278, 3219–3224.
- 953 McLeroy, C.A., Anderson, R.Y., 1966. Laminations of the Oligocene Florissant lake deposits,
- Colorado. Geological Society of America Bulletin 77, 605–618.
- Meyer, W., Seiler, T.B., Christ, A., Redelstein, R., Püttmann, W., Hollert, H., Achten, C., 2014.
- Mutagenicity, dioxin-like activity and bioaccumulation of alkylated picene and chrysene
- derivatives in a German lignite. Science of the Total Environment 497, 634–641.
- Meyers, P.A., 1997. Organic geochemical proxies of paleoceanographic, paleolimnologic, and
- paleoclimatic processes. Organic Geochemistry 27, 213–250.
- Moss, P.T., Greenwood, D.R., Archibald, S.B., 2005. Regional and local vegetation community
- 961 dynamics of the Eocene Okanagan Highlands (British Columbia-Washington State) from

- palynology. Canadian Journal of Earth Sciences 42, 187–204.
- Murray, A.P., Edwards, D., Hope, J.M., Boreham, C.J., Booth, W.E., Alexander, R.A.,
- Summons, R.E., 1998. Carbon isotope biogeochemistry of plant resins and derived
- hydrocarbons. Organic Geochemistry 29, 1199–1214.
- Noble, R.A., Alexander, R., Kagi, R.I., Knox, J., 1985. Tetracyclic diterpenoid hydrocarbons in
- some Australian coals, sediments and crude oils. Geochimica et Cosmochimica Acta 49,
- 968 2141–2147.
- Noble, R.A., Alexander, R., Kagi, R.I., Nox, J.K., 1986. Identification of some diterpenoid
- hydrocarbons in petroleum. Organic Geochemistry 10, 825–829.
- 971 Nytoft, H.P., Kildahl-Andersen, G., Lindström, S., Rise, F., Bechtel, A., Mitrović, D., Đoković,
- N., Životić, D., Stojanović, K.A., 2019. Dehydroicetexanes in sediments and crude oils:
- Possible markers for Cupressoideae. Organic Geochemistry 129, 14–23.
- Otto, A., Simoneit, B.R.T., 2001. Chemosystematics and diagenesis of terpenoids in fossil
- conifer species and sediment from the Eocene Zeitz formation, Saxony, Germany.
- 976 Geochimica et Cosmochimica Acta 65, 3505–3527.
- Otto, A., Walther, H., Püttmann, W., 1997. Sesqui- and diterpenoid biomarkers preserved in
- 978 Taxodium-rich oligocene oxbow lake clays, Weisselster basin, Germany. Organic
- 979 Geochemistry 26, 105–115.
- Otto, A., Simoneit, B.R.T., Rember, W.C., 2005. Conifer and angiosperm biomarkers in clay
- 981 sediments and fossil plants from the Miocene Clarkia Formation, Idaho, USA. Organic
- 982 Geochemistry 36, 907–922.
- Pagani, M., Pedentchouk, N., Huber, M., Sluijs, A., Schouten, S., Brinkhuis, H., Sinninghe
- Damsté, J.S., Dickens, G.R., Backman, J., Clemens, S., Cronin, T., Eynaud, F., Gattacceca, J.,

- Jakobsson, M., Jordan, R., Kaminski, M., King, J., Koc, N., Martinez, N.C., McInroy, D.,
- Moore, T.C., O'Regan, M., Onodera, J., Pälike, H., Rea, B., Rio, D., Sakamoto, T., Smith,
- D.C., St John, K.E.K., Suto, I., Suzuki, N., Takahashi, K., Watanabe, M., Yamamoto, M.,
- 988 2006. Arctic hydrology during global warming at the Palaeocene/Eocene thermal maximum.
- 989 Nature 442, 671–675.
- Pedentchouk, N., Sumner, W., Tipple, B., Pagani, M., 2008.  $\delta^{13}$ C and  $\delta D$  compositions of n-
- alkanes from modern angiosperms and conifers: An experimental set up in central
- Washington State, USA. Organic Geochemistry 39, 1066–1071.
- Peters, K.E., Walters, C.C., Moldowan, J.M., 2005. The Biomarker Guide, vol. 1.
- 994 Cambridge University Press, Cambridge, United Kingdom.
- 995 Philp, R.P., 1985. Fossil Fuel Biomarkers: Applications and Sprectra. Elsevier, New York.
- 996 Polissar, P.J., Freeman, K.H., 2010. Effects of aridity and vegetation on plant-wax δD in modern
- lake sediments. Geochimica et Cosmochimica Acta 74, 5785–5797.
- Polissar, P.J., Freeman, K.H., Rowley, D.B., McInerney, F.A., Currie, B.S., 2009. Paleoaltimetry
- of the Tibetan Plateau from D/H ratios of lipid biomarkers. Earth and Planetary Science
- 1000 Letters 287, 64–76.
- 1001 Powell, T.G., McKirdy, D.M., 1973. Relationship between ratio of pristane to phytane, crude oil
- 1002 composition and geological environment in Australia. Nature Physical Science 243, 37–39.
- Reichgelt, T., D'Andrea, W.J., Fox, B.R.S., 2016. Abrupt plant physiological changes in
- southern New Zealand at the termination of the Mi-1 event reflect shifts in hydroclimate and
- pCO<sub>2</sub>. Earth and Planetary Science Letters 455, 115–124.
- Rullkötter, J., Peakman, T.M., ten Haven, H.L., 1994. Early diagenesis of terrigenous
- triterpenoids and its implications for petroleum geochemistry. Organic Geochemistry 21,

- 1008 215–233.
- Rybicki, M., Marynowski, L., Simoneit, B.R., 2020. Composition of organic compounds from
- low-temperature burning of lignite and their application as tracers in ambient air.
- 1011 Chemosphere 249, 126087.
- Sachse, D., Billault, I., Bowen, G.J., Chikaraishi, Y., Dawson, T.E., Feakins, S.J., Freeman,
- 1013 K.H., Magill, C.R., McInerney, F.A., van der Meer, M.T.J., Polissar, P., Robins, R.J., Sachs,
- J.P., Schmidt, H.-L., Sessions, A.L., White, J.W.C., West, J.B., Kahmen, A., 2012. Molecular
- paleohydrology: Interpreting the hydrogen-isotopic composition of lipid biomarkers from
- photosynthesizing organisms. Annual Review of Earth and Planetary Sciences 40, 221–249.
- Sauer, P.E., Eglinton, T.I., Hayes, J.M., Schimmelmann, A., Sessions, A.L., 2001. Compound-
- specific D/H ratios of lipid biomarkers from sediments as a proxy for environmental and
- climatic conditions. Geochimica et Cosmochimica Acta 65, 213–222.
- 1020 Schouten, S., Woltering, M., Rijpstra, W.I.C., Sluijs, A., Brinkhuis, H., Sinninghe Damsté, J.S.,
- 1021 2007. The Paleocene-Eocene carbon isotope excursion in higher plant organic matter:
- Differential fractionation of angiosperms and conifers in the Arctic. Earth and Planetary
- 1023 Science Letters 258, 581–592.
- Simoneit, B.R.T., 1977. Diterpenoid compounds and other lipids in deep-sea sediments and their
- geochemical significance. Geochimica et Cosmochimica Acta 41, 463–476.
- Simoneit, B.R., Grimalt, J.O., Wang, T.G., Cox, R.E., Hatcher, P.G., Nissenbaum, A., 1986.
- 1027 Cyclic terpenoids of contemporary resinous plant detritus and of fossil woods, ambers and
- coals. Organic Geochemistry 10, 877-889.
- Smith, F.A., Wing, S.L., Freeman, K.H., 2007. Magnitude of the carbon isotope excursion at the
- Paleocene-Eocene thermal maximum: The role of plant community change. Earth and

- Planetary Science Letters 262, 50–65.
- Smith, R.Y., Basinger, J.F., Greenwood, D.R., 2012. Early Eocene plant diversity and dynamics
- in the Falkland flora, Okanagan Highlands, British Columbia, Canada. Palaeobiodiversity and
- Palaeoenvironments 92, 309–328.
- Stefanova, M., Magnier, C., 1997. Aliphatic biological markers in Miocene Maritza-Iztok lignite,
- Bulgaria. European Coal Geology and Technology 125, 219–228.
- Stefanova, M., Markova, K., Marinov, S., Simoneit, B.R.T., 2005. Molecular indicators for coal-
- forming vegetation of the Miocene Chukurovo lignite, Bulgaria. Fuel 84, 1830–1838.
- Stout, S.A., 1992. Aliphatic and aromatic triterpenoid hydrocarbons in a Tertiary angiospermous
- lignite. Organic Geochemistry 18, 51–66.
- ten Haven, H.L., de Leeuw, J.W., Rullkötter, J., Sinninghe Damsté, J.S., 1987. Restricted utility
- of the pristane/phytane ratio as a palaeoenvironmental indicator. Nature 330, 641–643.
- ten Haven, H.L., Peakman, T.M., Rullkötter, J., 1992. Early diagenetic transformation of higher-
- plant triterpenoids in deep-sea sediments from Baffin Bay. Geochimica et Cosmochimica
- 1045 Acta 56, 2001–2024.
- 1046 Tipple, B.J., Pagani, M., Krishnan, S., Dirghangi, S.S., Galeotti, S., Agnini, C., Giusberti, L.,
- Rio, D., 2011. Coupled high-resolution marine and terrestrial records of carbon and
- hydrologic cycles variations during the Paleocene Eocene Thermal Maximum (PETM).
- Earth and Planetary Science Letters 311, 82–92.
- 1050 Tissot, B.P., Welte, D.H., 1984. Petroleum Formation and Occurrence. Springer
- 1051 Verlag, Heidelberg.
- 1052 Trendel, J.M., Lohmann, F., Kintzinger, J.P., Albrecht, P., Chiarone, A., Riche, C., Cesario, M.,
- Guilhem, J., Pascard, C., 1989. Identification of des-A-triterpenoid hydrocarbons occurring in

- surface sediments. Tetrahedron 45, 4457–4470.
- Tuo, J., Philp, R.P., 2005. Saturated and aromatic diterpenoids and triterpenoids in Eocene coals
- and mudstones from China. Applied Geochemistry 20, 367–381.
- Wakeham, S.G., Schaffner, C., Giger, W., 1980. Polycyclic aromatic hydrocarbons in Recent
- lake sediments–II. Compounds derived from biogenic precursors during early diagenesis.
- Geochimica et Cosmochimica Acta 44, 415–429.
- 1060 West, C.K., Greenwood, D.R., Basinger, J.F., 2015. Was the Arctic Eocene "rainforest"
- monsoonal? Estimates of seasonal precipitation from early Eocene megafloras from Ellesmere
- Island, Nunavut. Earth and Planetary Science Letters 427, 18–30.
- 1063 West, C.K., Greenwood, D.R., Basinger, J.F., 2019. The late Paleocene and early Eocene Arctic
- megaflora of Ellesmere and Axel Heiberg islands, Nunavut, Canada. Palaeontographica
- 1065 Abteilung B 300, 47–163.
- 1066 West, C.K., Greenwood, D.R., Reichgelt, T., Lowe, A.J., Vachon, J.M., Basinger, J.F., 2020.
- Paleobotanical proxies for early Eocene climates and ecosystems in northern North America
- from mid to high latitudes, Climate of the Past Discussions, https://doi.org/10.5194/cp-2020-
- 1069 32.
- Williford, K.H., Grice, K., Holman, A., McElwain, J.C., 2014. An organic record of terrestrial
- ecosystem collapse and recovery at the Triassic Jurassic boundary in East Greenland.
- Geochimica et Cosmochimica Acta 127, 251–263.
- 1073 Wing, S.L., 1980. Fossil floras and plant-bearing beds of the central Bighorn Basin. In:
- Gingerich, P.D. (Ed.), Early Cenozoic Paleontology and Stratigraphy of the Bighorn Basin,
- Wyoming. University of Michigan Papers on Paleontology, pp. 119–125.
- 1076 Wing, S.L., 1984. Relation of paleovegetation to geometry and cyclicity of some fluvial

1077	carbonaceous deposits. Journal of Sedimentary Petrology 54, 52-66.
1078	Wing, S.L., Alroy, J., Hickey, L.J., 1995. Plant and mammal diversity in the Paleocene to early
1079	Eocene of the Bighorn Basin. Palaeogeography, Palaeoclimatology, Palaeoecology 115, 117-
1080	155.
1081	Wolfe, J.A., Schorn, H.E., 1989. Paleocologic, paleoclimatic, and evolutionary significance of
1082	the Oligocene Creede flora, Colorado. Paleobiology 15, 180–198.
1083	Wolfe, J.A., Schorn, H.E., 1990. Taxonomic revision of the Spermatopsida of the Oligocene
1084	Creede flora, southern Colorado. United States Geological Survey Bulletin 1923, 1–40.
1085	Wolff, G.A., Trendel, J.M., Albrecht, P., 1989. Novel monoaromatic triterpenoid hydrocarbons
1086	occuring in sediments. Tetrahedron 45, 6721–6728.
1087	Woolhouse, A.D., Oung, J.N., Philp, R.P., Weston, R.J., 1992. Triterpanes and ring-A degraded
1088	triterpanes as biomarkers characteristic of Tertiary oils derived from predominantly higher
1089	plant sources. Organic Geochemistry 18, 23–31.
1090	
1091	
1092	Figure Captions
1093	
1094	Fig. 1. Map of North America showing the paleobotanical sites where sediments were sampled.
1095	Points are numbered with a corresponding key to the right of the map, grouped by region. Light
1096	green points indicate angiosperm sites; dark green, conifer and mixed conifer sites. Panel (a)
1097	provides an expanded map for Ellesmere and Axel Heiberg islands; Panel (b), the Bighorn Basin
1098	

Fig. 2. Box and whisker plots of paleobotanical sites grouped by angiosperm sites (light green) and conifers/mixed conifer sites (dark green), then by age for: (a) Pr/Ph ratios; (b) carbon preference index (CPI); (c) terrestrial to aquatic ratios (TAR); and (d) average chain length (ACL'). Box and whisker plots show the median, upper and lower quartiles, and maximum and minimum values, with outlier values shown as black-filled symbols. Each point represents one sample, and different symbols represent distinct depositional environments. Letters on y-axis represent locations: Paleocene Bighorn Basin (A), Eocene Bighorn Basin (B), Florissant (C), late Paleocene/early Eocene Arctic coal swamp (D), late Paleocene/early Eocene Arctic floodplain (E), Driftwood Canyon coal swamp (F), Driftwood Canyon lacustrine (G), middle Eocene Arctic (H), Creede (I).

**Fig. 3.** Pie charts depicting the relative abundances of each biomarker: triterpenoids (light green); diterpenoids (dark green); and *n*-alkanes (purple). Here we show that sites with higher abundances of angiosperms (A–C) have higher amounts of *n*-alkanes (78.4–98.9%) compared to conifer and mixed conifer sites (D–I) (3.9–79.1%).

**Fig. 4.** Measured  $\delta^{13}$ C values of triterpenoids, diterpenoids, and *n*-alkanes from modern angiosperms and conifers (yellow) and from Paleogene angiosperms paleobotanical sites (light green; A–C) and conifer and mixed conifer paleobotanical sites (dark green; D–I). Modern biomarker  $\delta^{13}$ C values are from Diefendorf et al. (2012; 2015b; 2019); and Paleocene/Eocene Bighorn Basin sites are from Diefendorf et al. (2015a). To account for differences in atmospheric  $\delta^{13}$ C values between locations and for ease of comparison,  $\delta^{13}$ C values are plotted relative to *n*-C<sub>29</sub> alkanes for each site (orange shaded bar). Error bars represent 1σ for all species measured

(modern) or all biomarkers measured at each location (geologic sites). For each geologic site, the number of individual paleobotanical sites is denoted by n, and representative conifer taxa are listed. In modern angiosperms,  $\delta^{13}$ C values show little variation between chain lengths. In contrast, the  $\delta^{13}$ C values of n-alkanes increase with increasing chain length for modern Cupressaceae, Pinaceae, and Taxaceae conifers. This distinct conifer pattern is broadly conserved at geologic sites dominated by conifers (D, E, G). Long chain length n-alkanes homologues ( $C_{33}$  and  $C_{35}$ ) also show the highest conifer contribution at most conifer-dominated geologic sites (D–H) and at some angiosperm-dominated geologic sites (A and C), indicating that conifers may be contributing to these longer chain lengths even when not the dominant taxa.

**Fig. 5.** Box and whicker plots for  $\delta^{13}$ C<sub>leaf</sub> values calculated from triterpenoids (light green), diterpenoids (dark green), and n-C<sub>27</sub> to n-C<sub>35</sub> alkanes (purple). Box and whisker plots show the median, upper, and lower quartiles, and maximum and minimum values, with outlier values shown as black points.  $\delta^{13}$ C<sub>leaf</sub> values calculated from triterpenoids represent angiosperm leaf end members (green shaded region) and  $\delta^{13}$ C<sub>leaf</sub> values calculated from diterpenoids represent conifer leaf end member values (blue shaded regions) in sediment samples for each site (A–I). Dashed shaded regions represent estimated end member values where terpenoids were not detectable and are based on terpenoid values from similar locations when available (D, G) or a 3‰ offset (C, I). The  $\delta^{13}$ C<sub>leaf</sub> values of n-alkanes plotting within the range of angiosperm end members demonstrate sediment n-alkanes that are sourced from angiosperms (A–C) and  $\delta^{13}$ C<sub>leaf</sub> values of n-alkanes plotting within the range of conifer end members represent sediment n-alkanes sourced from conifers (H, I). Our data reveal that conifer contribution can be complex and vary by chain length. In some cases, n-alkanes represent a fairly mixed source of both angiosperms and

- 1145 conifers (F, G), but conifer input can also increase with increasing chain length (D, E, G).
- Therefore, it important to measure  $\delta^{13}$ C values for all long chain *n*-alkanes when using this
- method to help recognize the effects of paleovegetation.

Figure 1

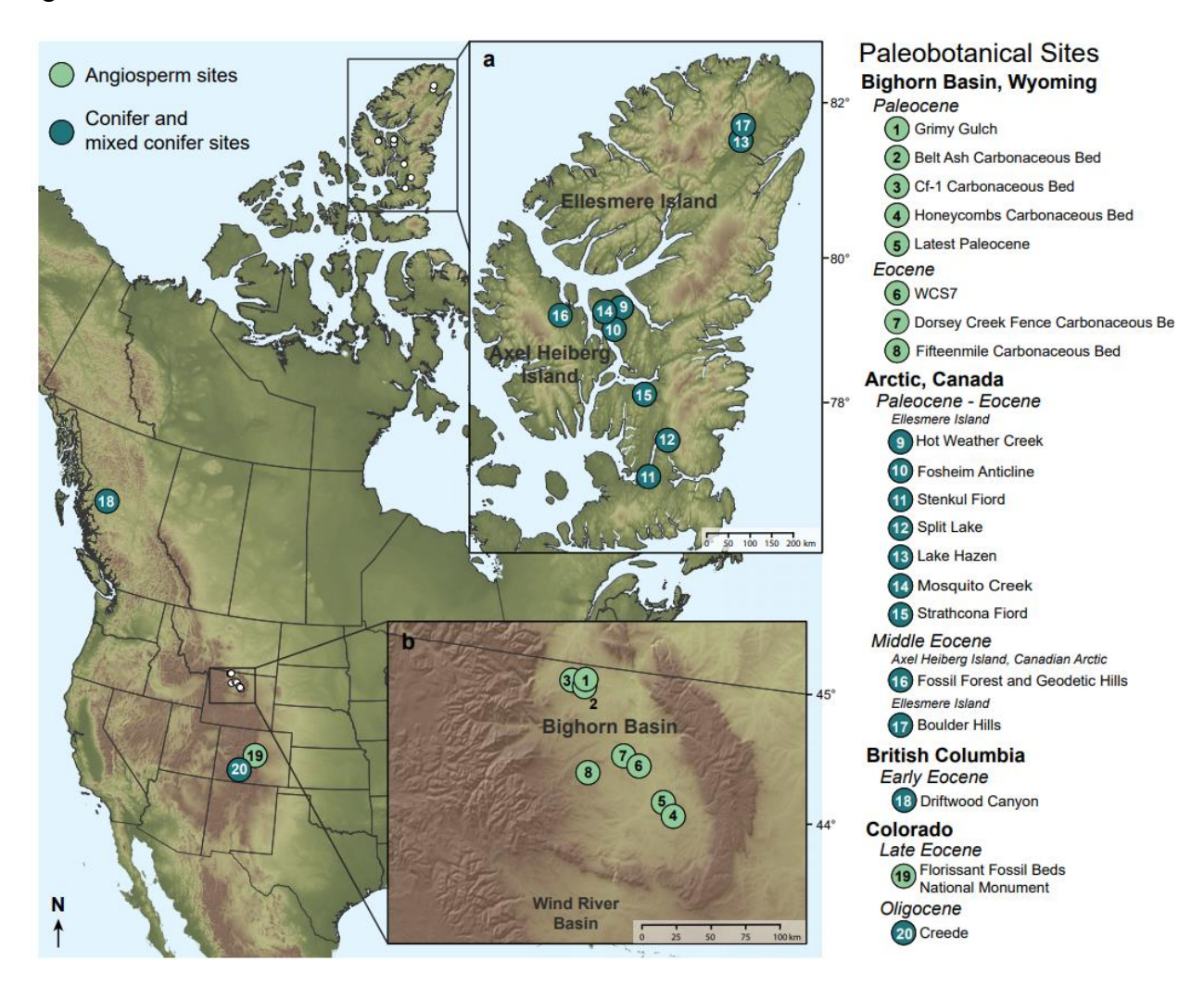


Figure 2

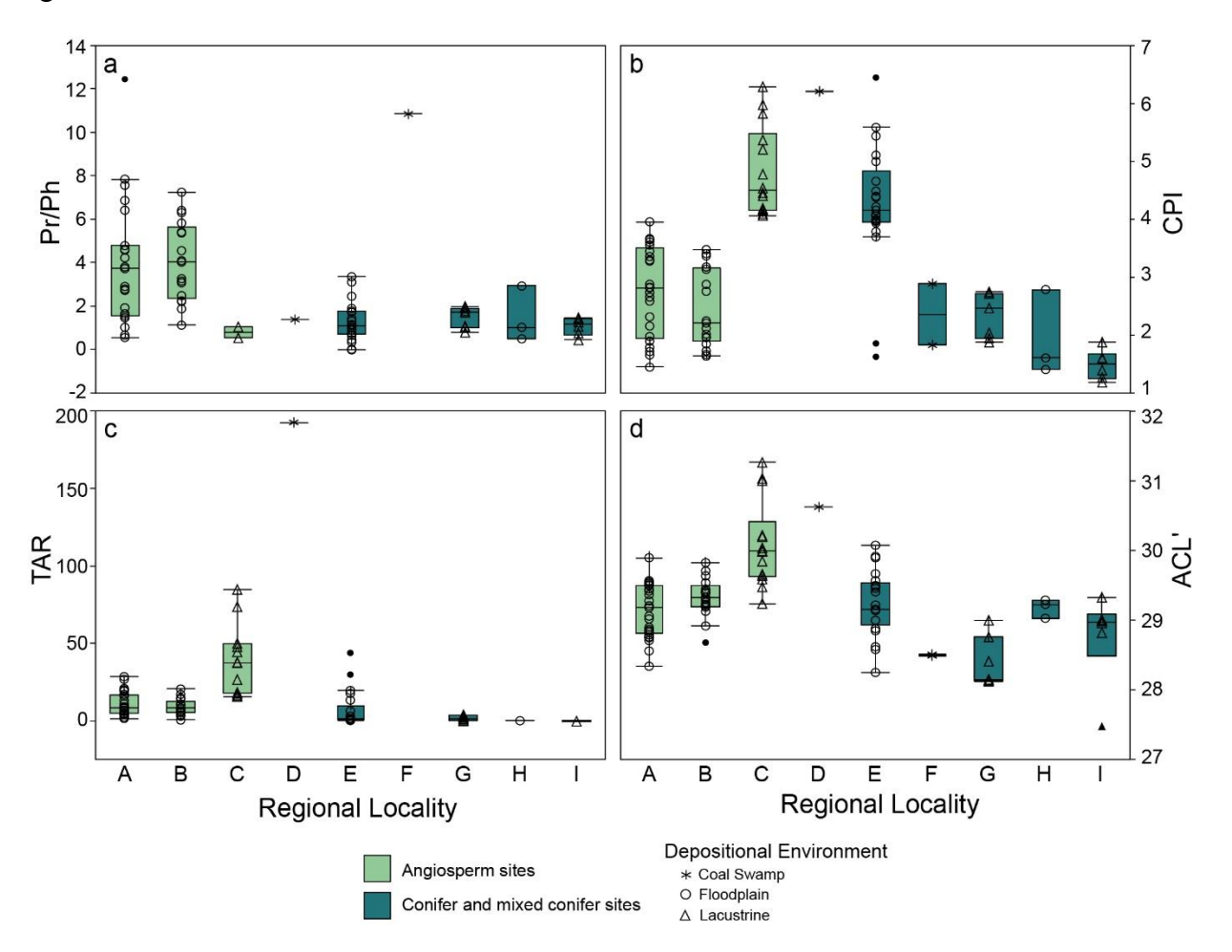


Figure 3

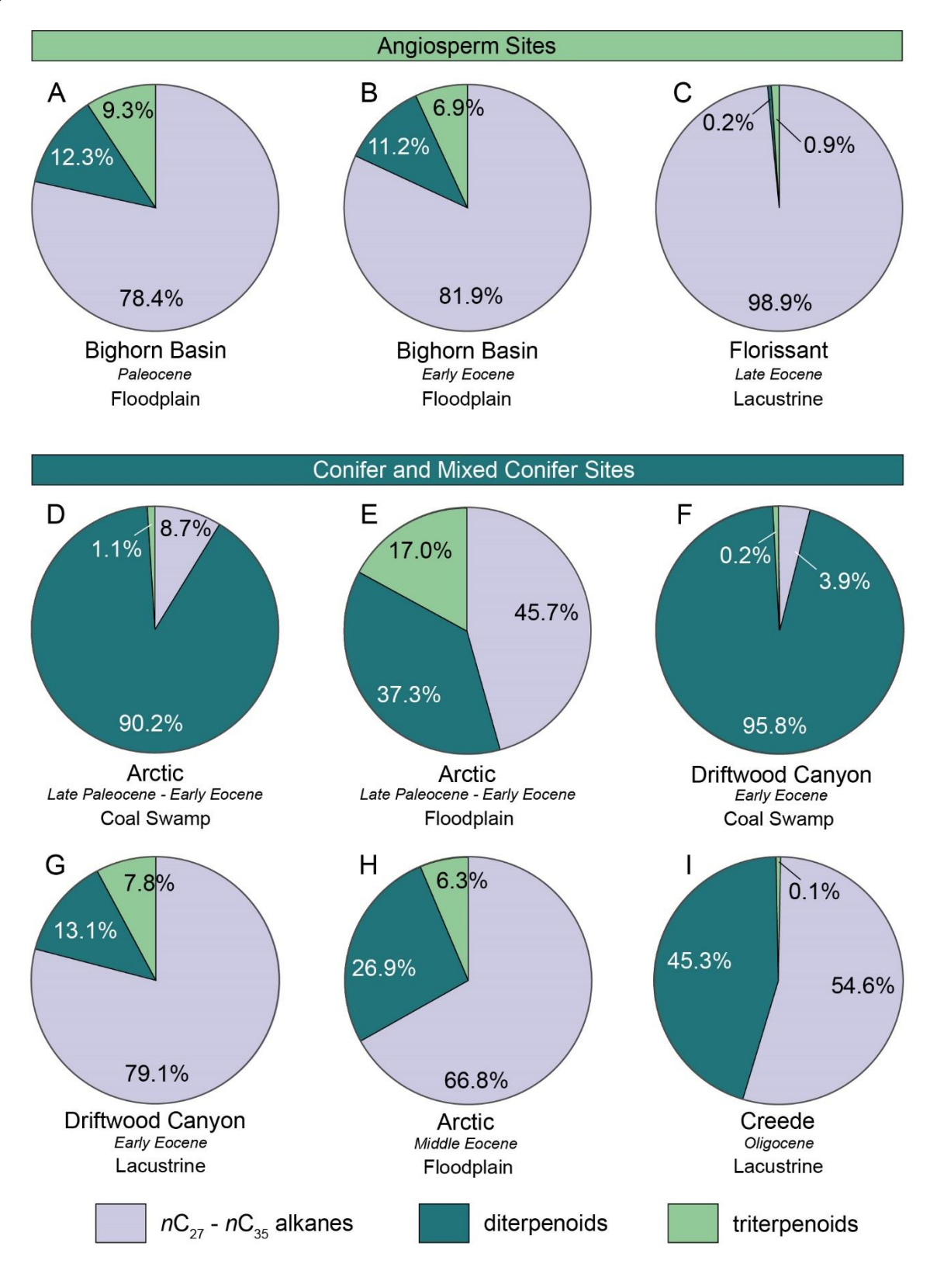


Figure 4

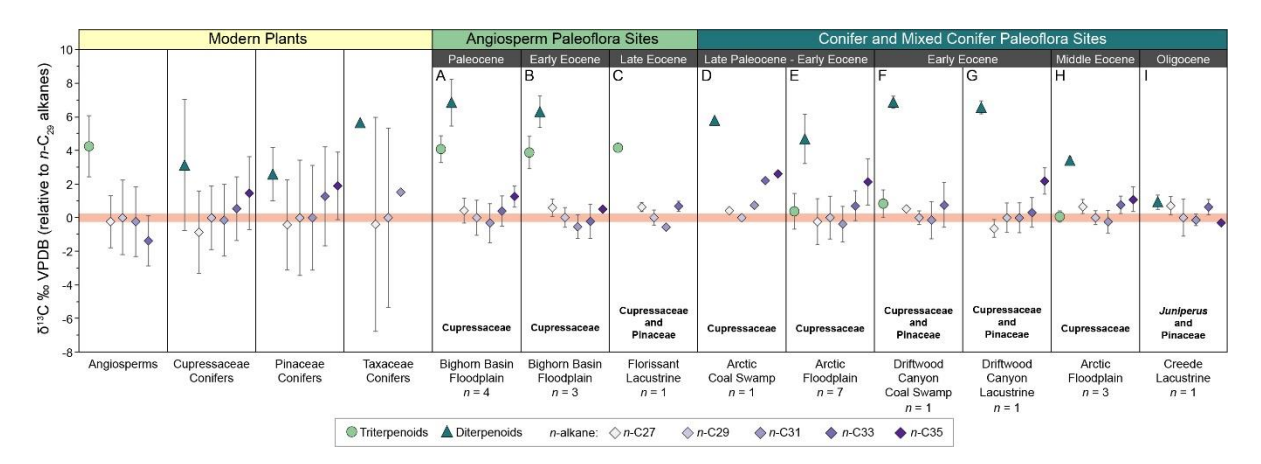
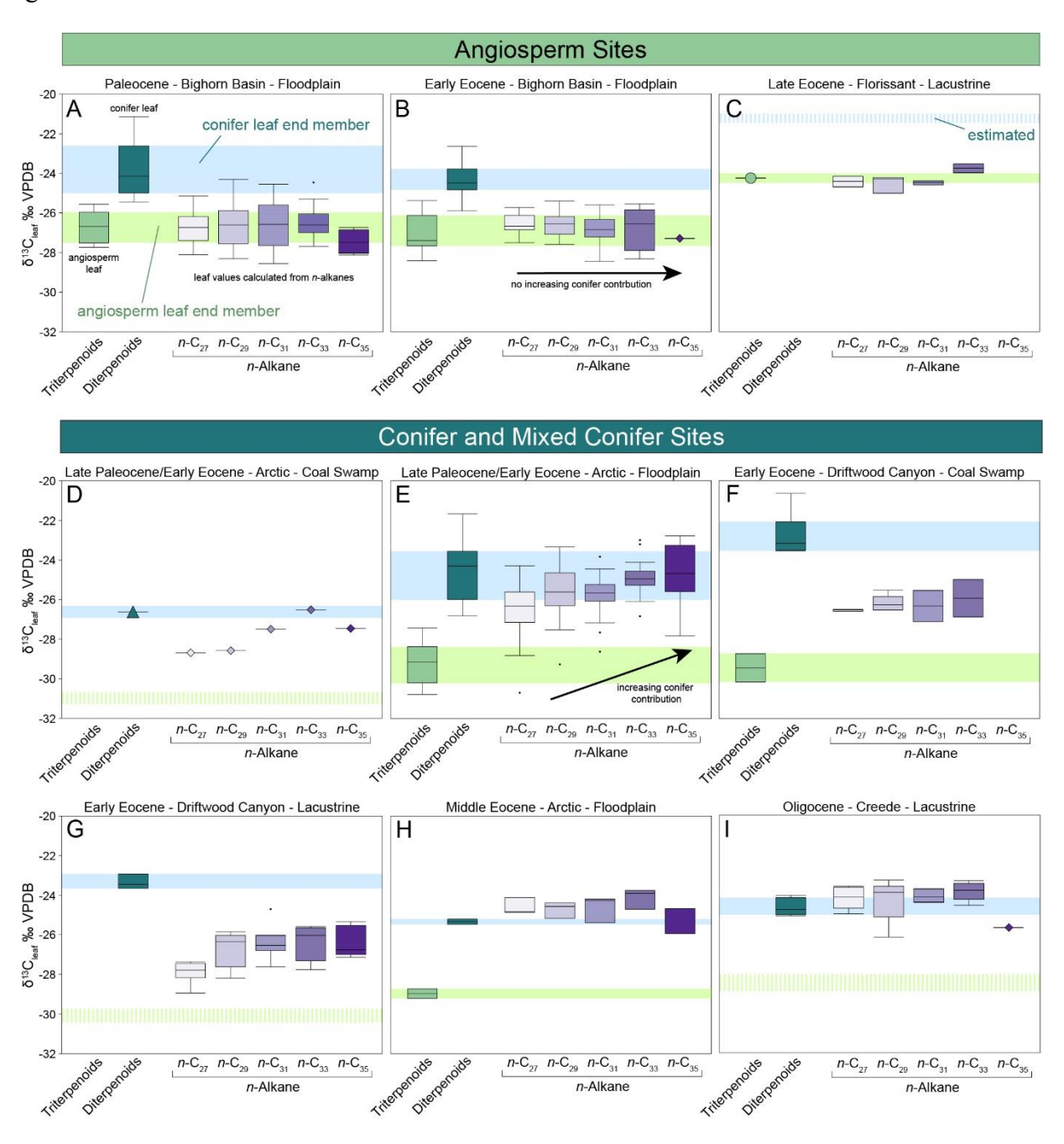


Figure 5



**Table 1**Regional localities with paleobotanical sites and site information including age, depositional environment, conifer paleovegetation, and paleobotanical references. Letters correspond to sites indicated in Figs. 2, 3, 4, and 5.

Regional Locality Paleobotanical Sites		Location	Age (Ma)	Depositional Environment	Paleovegetation (macrofossils)	Conifers (macrofossils)	Selected Paleobotanical References	
Paleocene								
(A) Bighorn Basin	Grimy Gulch, Belt Ash, Cf-1, Honeycombs, Latest Paleocene	Wyoming, USA	$63 \pm 1.5 - 56.04 \pm 1.5$	Floodplain	Angiosperm dominated, minor conifers	Metasequoia, Glyptostrobus	Davies-Vollum and Wing 1998; Smith et al., 2007; Diefendorf et al., 2014; Diefendorf et al., 2015a	
Late Paleocene -Ea	rly Eocene						,	
(D) Arctic	Stenkul Fiord	Ellesmere Island, Canada	55.5 - 53.1	Coal Swamp	Mixed broadleaf and conifer forest	Metasequoia, Glyptostrobus,	Eberle and Greenwood, 2012; West et al., 2015; West et al., 2019	
(E) Arctic	Hot Weather Creek, Fosheim Anticline, Stenkul Fiord, Split Lake, Lake Hazen, Mosquito Creek, Strathcona Fiord	Ellesmere Island, Canada	$57.6 \pm 1.6 - 51.9 \pm 4.1$	Floodplain	Mixed broadleaf and conifer forest	Metasequoia, Glyptostrobus,	Eberle and Greenwood, 2012; West et al., 2015; West et al., 2019	
Early Eocene	,							
(B) Bighorn Basin	WCS7, Dorsey Creek Fence, Fifteenmile Creek	Wyoming, USA	$55.35 \pm 1.5 -$ $52.98 \pm 1.5$	Floodplain	Angiosperm dominated, minor conifers	Metasequoia, Glyptostrobus	Davies-Vollum and Wing 1998; Smith et al., 2007; Diefendorf et al., 2014; Diefendorf et al., 2015a	
(F) Driftwood Canyon	Driftwood Canyon	British Columbia, Canada	$51.77 \pm 0.34$	Coal Swamp	Mixed broadleaf and conifer forest	Metasequoia, Sequoia, Chamaecyparis, Thuja, Pinaceae	Eberle et al., 2014	
(G) Driftwood Canyon	Driftwood Canyon	British Columbia, Canada	$51.77 \pm 0.34$	Lacustrine	Mixed broadleaf and conifer forest	Metasequoia, Sequoia, Chamaecyparis, Thuja, Pinaceae	Eberle et al., 2014	
Middle Eocene						1 maccae		
(H) Arctic	Boulder Hills, Fossil Forest, Geodetic Hills	Ellesmere and Axel Heiberg islands, Canada	$44.5 \pm 3.3 - 42.9 \pm 4.9$	Floodplain	Mixed broadleaf and conifer forest	Metasequoia, Glyptostrobus, Chamaecyparis, Pinaceae	McIver and Basinger, 1999; Eberle and Greenwood, 2012	
Late Eocene	Late Eocene						,	
(C) Florissant	Florissant	Florissant Fossil Beds National Monument, Colorado, USA	$34.07 \pm 0.1$	Lacustrine	Angiosperm dominated, minor conifers	Sequoia, Chamaecyparis, Torreya, Abies, Picea, Pinus	MacGinite, 1953; Gregory, 1994; Manchester, 2001	
Oligocene	Oligocene							
(I) Creede	Creede	Colorado, USA	$26.59 \pm 0.33$	Lacustrine	Conifer scrubland	Juniperus, Abies, Picea, Pinus	Wolfe and Schorn, 1989; Leopold and Zaborac- Reed, 2019	

Table 2
List of compounds used in this study with mass spectral data and references.

#	Saturation	Compound Name	Formula	Class	MW	Characteristic ion fragments $m/z^*$	Source
		DITERPENOIDS					
1	Aliphatic	Isonorpimarane	$C_{19}H_{34}$	Pimarane	262	233, 109, 123	Noble et al. (1986)
2	Aliphatic	Norpimarane	$C_{19}H_{34}$	Pimarane	262	233, 123, 109	Philp (1985)
3	Aliphatic	18-Norisopimarane	$C_{19}H_{34}$	Pimarane	262	233, 123, 109, 262, 245	Killops et al. (1995)
4	Aliphatic	Tetracyclic diterpane	$C_{19}H_{32}$	Kaurane?	260	109, 260, 189, 231	Spectral interpretation
5	Aliphatic	ent-Beyerane	$C_{20}H_{34}$	Beyerane	274	123, 245, 259, 274, 189	Noble et al. (1985)
6	Aliphatic	13α(H)-Fichtelite	$C_{19}H_{34}$	Abietane	262	109, 191, 95, 81, 262, 247	Otto and Simoneit (2001)
7	Aromatic	19-Norabieta-8,11,13-triene	$C_{19}H_{28}$	Abietane	256	159, 241, 185, 256, 117	Simoneit (1977)
8	Aromatic	19-Norabieta-4,8,11,13- tetraene	$C_{19}H_{26}$	Abietane	254	197, 100, 249	Philp (1985)
9	Aromatic	19-Norabieta-3,8,11,13- tetraene	$C_{19}H_{26}$	Abietane	254	239, 254, 199, 117, 159	Philp (1985)
10	Aromatic	18-Norabieta-8,11,13-triene	$C_{19}H_{28}$	Abietane	256	159, 241, 185, 256, 213	Simoneit (1977)
11	Aliphatic	Isopimarane	$C_{20}H_{36}$	Pimarane	276	247, 123, 163, 109, 276, 261	Tuo and Philp (2005)
	-	•					• ` '
12	Aliphatic	Pimarane	$C_{20}H_{36}$	Pimarane	276	247, 163, 123	NIST (2008)
13	Aliphatic	Abietane	$C_{20}H_{36}$	Abietane	276	163, 191, 276, 261, 233	Philp (1985)
14	Aliphatic	<i>ent</i> -16β(H)-Kaurane	$C_{20}H_{34}$	Kaurane	274	123, 274, 259, 231	Noble et al. (1985)
15	Aromatic	ent-13-epi manoyl oxide	$C_{20}H_{34}O$	Labdane	290	257, 275, 192, 177	Demetzos et al. (2002)
16	Aromatic	2-Methyl-1-(4'- methylpentyl)-6-	$C_{20}H_{28}$	Abietane	268	197, 268, 253, 167	Stefanova et al. (2005)
10	Atomatic	isopropylnaphthalene	C <sub>20</sub> 11 <sub>28</sub>	Adictanc	200	197, 200, 233, 107	Stefanova et al. (2003)
17	Aromatic	Abieta-8,11,13-triene	$C_{20}H_{30}$	Abietane	270	255, 173, 159, 185	Philp (1985)
18	Aromatic	Dehydroicetexane	$C_{20}H_{30}$	Abietane	270	270, 255, 146, 131, 185	Willford et al. (2014); Nytoft et al. (2019)
19	Aromatic	1,2,3,4-Tetrahydroretene	$C_{18}H_{22}$	Abietane	238	223, 238, 181, 163	Philp (1985)
20	Aromatic	Simonellite	$C_{19}H_{24}$	Abietane	252	237, 195, 165, 178	Simoneit (1977); Wakeham et al. (1980)
21	Aromatic	Diaromatic tricyclic totarane	$C_{19}H_{24}$	Totarane	252	237, 179, 193, 165	Tuo and Philp (2005)
22	Aromatic	Retene	$C_{18}H_{18}$	Abietane	234	219, 234, 204	Wakeham et al. (1980); Philp (1985)
		TRITERPENOIDS					
23	Aliphatic	Des-A-lupane	$C_{24}H_{42}$	Lupane	330	123, 109, 95, 163, 149, 191, 287, 315	Philp (1985); Stefanova and Magnier (1997)
24	Aromatic	Des-A-26-norlupa-5,7,9-triene	$C_{23}H_{34}$	Lupane	310	295, 157, 131	Wolff et al. (1989); Freeman et al. (1994)
25	Aliphatic	Des-A-ursane	$C_{24}H_{42}$	Ursane	330	123, 163, 109, 149, 330, 287, 191, 315	Woolhouse et al. (1992)
26	Aromatic	Similar to monoaromatic- (A)-triterpenoid	$C_{27}H_{38}$	Oleanane	362	145, 158, 347	Stout (1992)
27	Aromatic	Similar to 24,25,26-trinor-lupa-1,3,5 (10),?-tetraene	$C_{27}H_{38}$	Lupane	362	145, 190, 172, 347	ten Haven et al. (1992)
28	Aromatic	Olean-11,13(18)-diene	$C_{30}H_{48}$	Oleanane	408	408, 69, 255, 293	NIST (2008)
29	Aromatic	Olean-18-ene	$C_{30}H_{50}$	Oleanane	410	204, 189, 177, 395, 410	NIST (2008)
30	Aromatic	Dinor-oleana( <i>ursa</i> )-1,3,5(10)-triene	$C_{28}H_{42}$	-	378	145, 157, 172	Jacob et al. (2007)
31	Aromatic	Unknown pentacyclic triterpenoid (coelutes with	$C_{27}H_{36}$	Oleanane	360	195, 207, 221	Chang et al. (1988)
32	Aromatic	Compound 30) Olean-12-ene	$C_{30}H_{50}$	Oleanane	410	218, 203, 191, 257	Philp (1985)
33		Tetramethyloctahydropicene		Oleanane	342		Wakeham et al. (1980)
23	Aromatic	isomer Tetranor-olean( <i>ursa</i> )-	$C_{26}H_{30}$	Olcallalle	342	342, 218, 243	vv akciiaiii ci al. (1980)
34	Aromatic	1,3,5(10),6,8,11,13,15- octaene	$C_{26}H_{28}$	-	340	255, 340, 270, 239, 325, 283	Chaffee et al. (1984); Stout (1992); Jacob et al. (2007)
35	Aromatic	2,2,4a, 9-Tetramethyl- 1,2,3,4,4a,5,6,14b- octahydropicene	$C_{26}H_{30}$	Oleanane	342	342, 257, 243, 228, 299, 215, 123	Wakeham et al 1980; Chaffee and Fookes (1988)
36	Aromatic	1,2,9-Trimethyl-1,2,3,4- tetrahydropicene	$C_{25}H_{24}$	Oleanane	324	324, 309, 279, 255	Wakeham et al. (1980); Meyer et al. (2014)
37	Aromatic	2,2,9-Trimethyl-1,2,3,4-tetrahydropicene	$C_{25}H_{24}$	Oleanane	324	324, 309, 252	Wakeham et al. (1980); Meyer et al. (2014)

<sup>\*</sup>Listed in highest abundance

**Table 3** Carbon isotope mixing models showing TITE-derived % conifer contribution of sediment n-alkanes for each location

	% conif	% conifer contribution to sediment <i>n</i> -alkanes									
Location (Depositional environment), Age*	n-C <sub>27</sub> alkane	1σ	n-C <sub>29</sub> alkane	1σ	n-C <sub>31</sub> alkane	1σ	n-C <sub>33</sub> alkane	1σ	n-C <sub>35</sub> alkane	1σ	
Angiosperm Sites											
A. Bighorn Basin (Floodplain), EP	0%	30.2	2%	24.4	3%	20.8	9%	15.3	0%	32.6	
B. Bighorn Basin (Floodplain), EP	18%	25.3	16%	29.9	8%	18.3	9%	27.1	0%	-	
C. Florissant (Lacustrine), late E	0%	-	0%	-	0%	-	16%	-	-	-	
Conifer Sites											
D. Arctic (Coal Swamp), late EP/early E	55%	-	58%	-	81%	-	100%	-	82%	-	
E. Arctic (Floodplain), late EP./early E	59%	10.4	77%	5.4	76%	14.2	94%	15.5	98%	13.7	
F. Arctic (Floodplain), middle E	100%	0.1	100%	0.1	100%	0.2	100%	0.2	100%	0.2	
G. DC (Coal Swamp), early E.	43%	0.1	49%	0.1	47%	0.2	52%	0.2	-	-	
H. DC (Lacustrine), early E.	32%	0.1	49%	0.1	55%	0.1	55%	0.1	55%	0.1	
I. Creede (Lacustrine), OL	100%	0.3	100%	0.5	100%	0.3	100%	0.3	65%	-	

<sup>\*</sup>Age abbreviations: EP = Paleocene, E = Eocene, OL = Oligocene